

**A Three site Higgsless model**

R. Sekhar Chivukula,<sup>\*</sup> Baradhwaj Coleppa,<sup>†</sup> Stefano Di Chiara,<sup>‡</sup> and Elizabeth H. Simmons<sup>§</sup>  
*Department of Physics and Astronomy, Michigan State University East Lansing, Michigan 48824, USA*

Hong-Jian He<sup>||</sup>

*Center for High Energy Physics, Tsinghua University Beijing 100084, China*

Masafumi Kurachi<sup>¶</sup>

*C.N. Yang Institute for Theoretical Physics, State University of New York Stony Brook, New York 11794, USA*

Masaharu Tanabashi<sup>\*\*</sup>

*Department of Physics, Tohoku University Sendai 980-8578, Japan*

(Received 17 July 2006; published 30 October 2006)

We analyze the spectrum and properties of a highly deconstructed Higgsless model with only three sites. Such a model contains sufficient complexity to incorporate interesting physics issues related to fermion masses and electroweak observables, yet remains simple enough that it could be encoded in a Matrix Element Generator program for use with Monte Carlo simulations. The gauge sector of this model is equivalent to that of the Breaking Electroweak Symmetry Strongly (BESS) model; the new physics of interest here lies in the fermion sector. We analyze the form of the fermion Yukawa couplings required to produce the ideal fermion delocalization that causes tree-level precision electroweak corrections to vanish. We discuss the size of one-loop corrections to  $b \rightarrow s\gamma$ , the weak-isospin violating parameter  $\alpha T$  and the decay  $Z \rightarrow b\bar{b}$ . We find that the new fermiophobic vector states (the analogs of the gauge-boson Kaluza-Klein modes in a continuum model) can be reasonably light, with a mass as low as 380 GeV, while the extra (approximately vectorial) quark and lepton states (the analogs of the fermion Kaluza-Klein modes) must be heavier than 1.8 TeV.

DOI: [10.1103/PhysRevD.74.075011](https://doi.org/10.1103/PhysRevD.74.075011)

PACS numbers: 12.60.Cn, 11.10.Kk

**I. INTRODUCTION**

Higgsless models [1] literally break the electroweak symmetry without invoking a scalar Higgs boson [2]. Among the most popular are models [3–6] based on a five-dimensional  $SU(2) \times SU(2) \times U(1)$  gauge theory in a slice of anti-de Sitter space, with electroweak symmetry breaking encoded in the boundary conditions of the gauge fields. The spectrum includes states identified with the photon,  $W$ , and  $Z$ , and also an infinite tower of additional massive vector bosons (the higher Kaluza-Klein or  $KK$  excitations) starting at the TeV scale [7], whose exchange unitarizes longitudinal  $W$  and  $Z$  boson scattering [8–11]. The properties of Higgsless models may be studied [12–18] by using the technique of deconstruction [19,20] and computing the precision electroweak parameters [21–25] in a related linear Moose model [26].

Our analysis of the leading electroweak parameters in a very general class of linear Moose models concluded [18] that a Higgsless model with localized fermions cannot simultaneously satisfy unitarity bounds and provide ac-

ceptably small precision electroweak corrections unless it includes light vector bosons other than the photon,  $W$ , and  $Z$ . Several authors proposed [27–30] that delocalizing fermions within the extra dimension could reduce electroweak corrections. In deconstructed language, delocalization means allowing fermions to derive electroweak properties from more than one site on the lattice of gauge groups [31,32]. We then showed [33] for an arbitrary Higgsless model that choosing the probability distribution of the delocalized fermions to be related to the wave function of the  $W$  boson makes three ( $\hat{S}$ ,  $\hat{T}$ ,  $W$ ) of the leading zero-momentum precision electroweak parameters defined by Barbieri, *et al.* [24,25] vanish at tree level. We denote such fermions as “ideally delocalized.” We subsequently provided a continuum realization of ideal delocalization that preserves the characteristic of vanishing precision electroweak corrections up to subleading order [34]. In the absence of precision electroweak corrections, the strongest constraints on Higgsless models come from limits on deviations in multi-gauge-boson vertices; we computed the general form of the triple and quartic gauge-boson couplings for these models and related them to the parameters of the electroweak chiral Lagrangian [35,36].

In this paper, we show that many issues of current interest, such as ideal fermion delocalization and the generation of fermion masses (including the top-quark mass) can be usefully illustrated in a Higgsless model decon-

<sup>\*</sup>E-mail: [sekhar@msu.edu](mailto:sekhar@msu.edu)

<sup>†</sup>E-mail: [baradhwa@msu.edu](mailto:baradhwa@msu.edu)

<sup>‡</sup>E-mail: [dichiara@msu.edu](mailto:dichiara@msu.edu)

<sup>§</sup>E-mail: [esimmons@msu.edu](mailto:esimmons@msu.edu)

<sup>||</sup>E-mail: [hjhe@mail.tsinghua.edu.cn](mailto:hjhe@mail.tsinghua.edu.cn)

<sup>¶</sup>E-mail: [masafumi.kurachi@stonybrook.edu](mailto:masafumi.kurachi@stonybrook.edu)

<sup>\*\*</sup>E-mail: [tanabash@tuhep.phys.tohoku.ac.jp](mailto:tanabash@tuhep.phys.tohoku.ac.jp)

structed to just three sites. The Moose describing the model has only one “interior”  $SU(2)$  group and there is, accordingly, only a single triplet of  $W'$  and  $Z'$  states instead of the infinite tower of triplets present in the continuum limit. This model contains sufficient complexity to incorporate the interesting physics issues, yet remains simple enough that it could be encoded in a Matrix Element Generator program in concert with a Monte Carlo Event Generator<sup>1</sup> for a detailed investigation of collider signatures.

The three-site model we introduce here has the color group of the Standard Model (SM) and an extended  $SU(2) \times SU(2) \times U(1)$  electroweak gauge group. This theory is in the same class as models of extended electroweak gauge symmetries [37,38] motivated by models of hidden local symmetry [39–43]. Indeed the gauge sector is precisely that of the BESS model [37]; the new physics discussed here relates to the fermion sector. In the next section of this paper we briefly describe the model and the limits in which we work. Section III reviews the gauge sector of the model in our notation, including the masses and wave functions of the photon, the nearly-standard light  $W$  and  $Z$ , and the heavier  $W'$  and  $Z'$ . Section IV solves for the masses and wave functions of the fermions in the spectrum (a set of SM-like fermions and heavy copies of those fermions) and implements ideal delocalization for the light fermions. Sections V and VI explore the couplings of the fermions to the charged and neutral gauge bosons, respectively. Because the light fermions are ideally delocalized, they lack couplings to the  $W'$  and  $Z'$ —and this minimizes the values of electroweak precision observables. The top-quark, on the other hand, is treated separately in order to provide for its large mass. The relationship of triple gauge vertices to ideal delocalization and a comparison of multigauge vertices in the three-site model and its continuum limit are discussed in Section VII; given the vanishing electroweak corrections and the fermiophobic nature of the  $W'$  and  $Z'$ , multigauge vertices offer the best prospects for additional experimental constraints on the three-site model. In Sections VIII and IX, the paper moves on to a discussion of  $\alpha T$  and the  $Zb\bar{b}$  vertex at one-loop. Having established that the heavy fermions must have masses of over 1.8 TeV, we discuss the structure of a low-energy effective theory in which those fermions have been integrated out. Section X presents our conclusions.

## II. THREE-SITE MODEL

The electroweak sector of the three-site Higgsless model analyzed in this paper is illustrated in Fig. 1 using “Moose notation”. The model incorporates a  $SU(2) \times SU(2) \times U(1)$  gauge group, and 2 nonlinear  $(SU(2) \times SU(2))/SU(2)$  sigma models in which the global symmetry groups in adjacent sigma models are identified with the corresponding factors of the gauge group. The symmetry break-

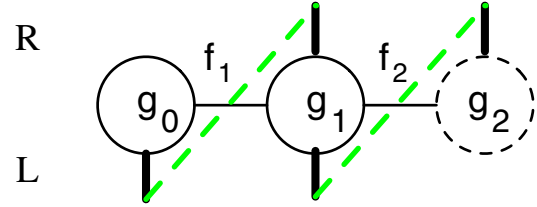


FIG. 1 (color online). The three-site model analyzed in this paper. The solid circles represent  $SU(2)$  gauge groups, with coupling strengths  $g_0$  and  $g_1$ , and the dashed circle is a  $U(1)$  gauge group with coupling  $g_2$ . The left-handed fermions, denoted by the lower vertical lines, are located at sites 0 and 1, and the right-handed fermions, denoted by the upper vertical lines, are at sites 1 and 2. The dashed green lines correspond to Yukawa couplings, as described in the text. As discussed below, we will take  $f_1 = f_2 = \sqrt{2}v$ , denote  $g_0 = g$ ,  $g_1 = \tilde{g}$ ,  $g_2 = g'$ , and take  $\tilde{g} \gg g, g'$ .

ing between the middle  $SU(2)$  and the  $U(1)$  follows a  $SU(2)_L \times SU(2)_R/SU(2)_V$  symmetry breaking pattern with the  $U(1)$  embedded as the  $T_3$ -generator of  $SU(2)_R$ . This extended electroweak gauge sector is that of the BESS model [37].

The left-handed fermions are  $SU(2)$  doublets coupling to the groups at the first two sites, which we will correspondingly label  $\psi_{L0}$  and  $\psi_{L1}$ . The right-handed fermions are a  $SU(2)$  doublet at site 1,  $\psi_{R1}$ , and two singlet fermions, denoted in Fig. 1 as “residing” at site 2,  $u_{R2}$  and  $d_{R2}$ . The fermions  $\psi_{L0}$ ,  $\psi_{L1}$ , and  $\psi_{R1}$  have  $U(1)$  charges typical of the left-handed doublets in the standard model,  $+1/6$  for quarks and  $-1/2$  for leptons. Similarly, the fermion  $u_{R2}$  has  $U(1)$  charges typical for the right-handed up-quarks ( $+2/3$ ), and  $d_{R2}$  has the  $U(1)$  charge associated with the right-handed down-quarks ( $-1/3$ ) or the leptons ( $-1$ ). With these assignments, we may write the Yukawa couplings and fermion mass<sup>2</sup> term

$$\begin{aligned} \mathcal{L}_f = & \lambda f_1 \bar{\psi}_{L0} \Sigma_1 \psi_{R1} + \sqrt{2} \tilde{\lambda} v \bar{\psi}_{R1} \psi_{L1} \\ & + f_2 \bar{\psi}_{L1} \Sigma_2 \begin{pmatrix} \lambda'_u & \\ & \lambda'_d \end{pmatrix} \begin{pmatrix} u_{R2} \\ d_{R2} \end{pmatrix} + \text{H.c.} \end{aligned} \quad (2.1)$$

Here we have chosen to write the  $\bar{\psi}_{R1} \psi_{L1}$  Dirac mass in the form of a Yukawa coupling, for convenience, and the matrices  $\Sigma_{1,2}$  are the nonlinear sigma-model fields associated with the  $f_{1,2}$  links of the Moose. The Yukawa couplings introduced here are of precisely the correct form required to implement a deconstruction of a five-dimensional fermion with chiral boundary conditions [44]. In the limit in which the “bulk fermion” decouples, while holding the mixing with the light fermions fixed, the model reduces to that considered in [45].

It is straightforward to incorporate quark flavor and mixing in a minimal way. Adding generational indices to

<sup>1</sup>See, e.g., those appearing on <http://www-theory.lbl.gov/tools/>.

<sup>2</sup>In this paper, we will not address the issue of nonzero neutrino masses. Our focus, instead, is on the physics related to the generation of the large top-quark mass.

each of the fermion fields, we may choose the coupling  $\lambda$  and the mass term  $\sqrt{2}\tilde{\lambda}v$  to be generation-diagonal. In this case, all of the nontrivial flavor structure is embedded in the Yukawa matrices  $\lambda'_u$  and  $\lambda'_d$ —precisely as in the standard model; the only mixing parameters that appear are the ordinary Cabibbo Kobayashi Maskawa (CKM) angles and phase. We focus most of our attention, in this paper, on the top-bottom quark doublet and its heavy partners, and we note where results for the other fermions differ.

For simplicity, we examine the case

$$f_1 = f_2 = \sqrt{2}v, \quad (2.2)$$

and work in the limit

$$x = g_0/g_1 \ll 1, \quad y = g_2/g_1 \ll 1, \quad (2.3)$$

in which case we expect a massless photon, light  $W$  and  $Z$  bosons, and a heavy set of bosons  $W'$  and  $Z'$ . Numerically, then,  $g_{0,2}$  are approximately equal to the standard model  $SU(2)_W$  and  $U(1)_Y$  couplings, and we therefore denote  $g_0 \equiv g$  and  $g_2 \equiv g'$ , and define an angle  $\theta$  such that

$$\frac{g'}{g} = \frac{\sin\theta}{\cos\theta} \equiv \frac{s}{c}. \quad (2.4)$$

In addition, we denote  $g_1 \equiv \tilde{g}$ .

In what follows, we will show that ideal mixing requires the flavor-independent mass contribution from  $\Sigma_1$  to be much smaller than the Dirac mass contribution:

$$\varepsilon_L \equiv \frac{\lambda}{\tilde{\lambda}} = \mathcal{O}(x) \ll 1. \quad (2.5)$$

While we will not immediately require that the flavor-dependent mass contributions associated with  $\Sigma_2$

$$\varepsilon_{uR,dR} \equiv \frac{\lambda'_{u,d}}{\tilde{\lambda}}, \quad (2.6)$$

be similarly small, we will ultimately find that they are bounded from above. The Yukawa and fermion mass terms in the Lagrangian can now be rephrased as

$$\begin{aligned} \mathcal{L}_f = \sqrt{2}\tilde{\lambda}v \left[ \varepsilon_L \bar{\psi}_{L0} \Sigma_1 \psi_{R1} + \bar{\psi}_{R1} \psi_{L1} \right. \\ \left. + \bar{\psi}_{L1} \Sigma_2 \begin{pmatrix} \varepsilon_{uR} & \\ & \varepsilon_{dR} \end{pmatrix} \begin{pmatrix} u_{R2} \\ d_{R2} \end{pmatrix} + \text{H.c.} \right] \quad (2.7) \end{aligned}$$

for easy reference.

Finally note that, treating the link fields as nonlinear sigma models, the model as described here is properly considered a low-energy effective theory valid below a mass scale of order  $4\pi\sqrt{2}v \approx 4.3$  TeV. If we regard each of the link fields as arising from QCD-like dynamics at that scale, we would expect large corrections to the  $S$  parameter arising from higher-energy operators [16]. On the other hand, if this model is viewed as the deconstructed form of a five-dimensional “dual” of some strongly

coupled four-dimensional theory [46–49], the leading corrections are accounted for by tree-level  $W'$ -exchange [5]. The remaining corrections are suppressed in the large- $N$  expansion, and may be sufficiently small to be phenomenologically acceptable.

### III. MASSES AND EIGENSTATES

This section reviews the mass eigenvalues and the wave functions of the gauge bosons of the three-site model, which are the same as those for the BESS model [37]. Ref. [12] has also previously discussed the gauge-boson eigenfunctions, but wrote them in terms of the parameters  $e$ ,  $M_W$ ,  $M_Z$ ,  $M_{W'}$ , and  $M_{Z'}$ .

#### A. Charged gauge bosons

The charged gauge boson mass-squared matrix may be written in terms of the small parameter  $x$  as

$$\frac{\tilde{g}^2 v^2}{2} \begin{pmatrix} x^2 & -x \\ -x & 2 \end{pmatrix}. \quad (3.1)$$

Diagonalizing this matrix perturbatively in  $x$ , we find the light eigenvalue

$$M_W^2 = \frac{\tilde{g}^2 v^2}{4} \left[ 1 - \frac{x^2}{4} + \frac{x^6}{64} + \dots \right], \quad (3.2)$$

and the corresponding eigenstate

$$\begin{aligned} W^\mu &= v_W^0 W_0^\mu + v_W^1 W_1^\mu \\ &= \left( 1 - \frac{x^2}{8} - \frac{5x^4}{128} + \dots \right) W_0^\mu \\ &\quad + \left( \frac{x}{2} + \frac{x^3}{16} - \frac{9x^5}{256} + \dots \right) W_1^\mu, \quad (3.3) \end{aligned}$$

where  $W_{0,1}$  are the gauge bosons associated with the  $SU(2)$  groups at sites 0 and 1. Note that the light  $W$  is primarily located at site 0.

The heavy eigenstate has an eigenvector orthogonal to that in Eq. (3.3) and a mass

$$M_{W'}^2 = \tilde{g}^2 v^2 \left[ 1 + \frac{x^2}{4} + \frac{x^4}{16} + \dots \right]. \quad (3.4)$$

Comparing Eqs. (3.2) and (3.4), we find

$$\frac{M_W^2}{M_{W'}^2} = \frac{x^2}{4} - \frac{x^4}{8} + \frac{x^6}{64} + \dots, \quad (3.5)$$

or, equivalently,

$$\left( \frac{g_0}{g_1} \right)^2 \equiv x^2 = 4 \left( \frac{M_W^2}{M_{W'}^2} \right) + 8 \left( \frac{M_W^2}{M_{W'}^2} \right)^2 + 28 \left( \frac{M_W^2}{M_{W'}^2} \right)^3 + \dots, \quad (3.6)$$

which confirms that the  $W'$  boson is heavy in the limit of small  $x$ .

### B. Neutral gauge bosons

The neutral bosons' mass-squared matrix is

$$\frac{\tilde{g}^2 v^2}{2} \begin{pmatrix} x^2 & -x & 0 \\ -x & 2 & -xt \\ 0 & -xt & x^2 t^2 \end{pmatrix}, \quad (3.7)$$

where  $t \equiv \tan\theta = s/c$ . This matrix has a zero eigenvalue, corresponding to the massless photon, with an eigenstate which may be written

$$A^\mu = \frac{e}{g} W_0^\mu + \frac{e}{\tilde{g}} W_1^\mu + \frac{e}{g'} B^\mu, \quad (3.8)$$

where  $W_{0,1}$  are the gauge bosons associated with the  $SU(2)$  groups at sites 0 and 1, the  $B$  is the gauge boson associated with the  $U(1)$  group at site 2, and the electric charge  $e$  satisfies

$$\frac{1}{e^2} = \frac{1}{g^2} + \frac{1}{\tilde{g}^2} + \frac{1}{g'^2}. \quad (3.9)$$

The light neutral gauge boson, which we associate with the  $Z$ , has a mass

$$M_Z^2 = \frac{g^2 v^2}{4c^2} \left[ 1 - \frac{x^2}{4} \frac{(c^2 - s^2)^2}{c^2} + \frac{x^6}{64} \frac{(c^2 - s^2)^4}{c^6} + \dots \right], \quad (3.10)$$

with a corresponding eigenvector

$$Z^\mu = v_Z^0 W_0^\mu + v_Z^1 W_1^\mu + v_Z^2 B^\mu \quad (3.11)$$

$$v_Z^0 = c - \frac{x^2 c^3 (1 + 2t^2 - 3t^4)}{8} + \dots \quad (3.12)$$

$$v_Z^1 = \frac{xc(1 - t^2)}{2} + \frac{x^3 c^3 (1 - t^2)^3}{16} + \dots \quad (3.13)$$

$$v_Z^2 = -s - \frac{x^2 s c^2 (3 - 2t^2 - t^4)}{8} + \dots \quad (3.14)$$

The heavy neutral boson has a mass

$$M_{Z'}^2 = \tilde{g}^2 v^2 \left[ 1 + \frac{x^2}{4c^2} + \frac{x^4 (1 - t^2)^2}{16} + \dots \right], \quad (3.15)$$

with the corresponding eigenvector

$$Z'^\mu = v_{Z'}^0 W_0^\mu + v_{Z'}^1 W_1^\mu + v_{Z'}^2 B^\mu \quad (3.16)$$

$$v_{Z'}^0 = -\frac{x}{2} - \frac{x^3 (1 - 3t^2)}{16} + \dots \quad (3.17)$$

$$v_{Z'}^1 = 1 - \frac{x^2 (1 + t^2)}{8} + \dots \quad (3.18)$$

$$v_{Z'}^2 = -\frac{xt}{2} + \frac{x^3 t (3 - t^2)}{16} + \dots \quad (3.19)$$

### IV. FERMION WAVE FUNCTIONS AND IDEAL DELOCALIZATION

This section analyzes the fermion sector of the three-site model and implements ideal fermion delocalization explicitly.

#### A. Fermion masses and wave functions

Consider the fermion mass matrix

$$M_{u,d} = \sqrt{2} \tilde{\lambda} v \begin{pmatrix} \varepsilon_L & 0 \\ 1 & \varepsilon_{uR,dR} \end{pmatrix} \equiv \begin{pmatrix} m & 0 \\ M & m'_{u,d} \end{pmatrix}. \quad (4.1)$$

The notation introduced at the far right is used to emphasize the ‘‘see-saw’’ form of the mass matrix. In what follows, we will largely be interested in the top- and bottom-quarks, and therefore in  $\varepsilon_{tR}$  and  $\varepsilon_{bR}$  (or, equivalently, in  $m'_t/M$  and  $m'_b/M$ ).

Diagonalizing the top-quark see-saw style mass matrix perturbatively in  $\varepsilon_L$ , we find the light eigenvalue

$$m_t = \frac{\sqrt{2} \tilde{\lambda} v \varepsilon_L \varepsilon_{tR}}{\sqrt{1 + \varepsilon_{tR}^2}} \left[ 1 - \frac{\varepsilon_L^2}{2(\varepsilon_{tR}^2 + 1)^2} + \dots \right], \quad (4.2)$$

$$\approx \frac{m m'_t}{\sqrt{M^2 + m_t'^2}}. \quad (4.3)$$

Note that this is precisely the same form as found in [30]. For the bottom-quark, we find the same expression with  $\varepsilon_{tR} \rightarrow \varepsilon_{bR}$ , and therefore (neglecting higher order terms in  $\varepsilon_{bR}^2$ )

$$\frac{m_b}{m_t} \approx \frac{\varepsilon_{bR}}{\varepsilon_{tR}} \sqrt{1 + \varepsilon_{tR}^2}. \quad (4.4)$$

The heavy eigenstate ( $T$ ) corresponding to the top-quark has a mass

$$m_T = \sqrt{2} \tilde{\lambda} v \sqrt{1 + \varepsilon_{tR}^2} \left[ 1 + \frac{\varepsilon_L^2}{2(\varepsilon_{tR}^2 + 1)^2} + \dots \right], \quad (4.5)$$

$$\approx \sqrt{M^2 + m_t'^2} \quad (4.6)$$

and similarly for the heavy eigenstate corresponding to the bottom-quark ( $B$ ) with  $\varepsilon_{tR} \rightarrow \varepsilon_{bR}$  (or, equivalently,  $m'_t \rightarrow m'_b$ ).

The left- and right-handed light mass eigenstates of the top-quark are

$$\begin{aligned} t_L &= t_L^0 \psi_{L0}' + t_L^1 \psi_{L1}' \\ &= \left( -1 + \frac{\varepsilon_L^2}{2(1 + \varepsilon_{tR}^2)^2} + \frac{(8\varepsilon_{tR}^2 - 3)\varepsilon_L^4}{8(\varepsilon_{tR}^2 + 1)^4} + \dots \right) \psi_{L0}' \\ &\quad + \left( \frac{\varepsilon_L}{1 + \varepsilon_{tR}^2} + \frac{(2\varepsilon_{tR}^2 - 1)\varepsilon_L^3}{2(\varepsilon_{tR}^2 + 1)^3} + \dots \right) \psi_{L1}' \end{aligned} \quad (4.7)$$

$$\begin{aligned}
 t_R &= t_R^1 \psi_{R1}' + t_R^2 t_{R2} \\
 &= \left( -\frac{\varepsilon_{iR}}{\sqrt{1 + \varepsilon_{iR}^2}} + \frac{\varepsilon_{iR} \varepsilon_L^2}{(1 + \varepsilon_{iR}^2)^{5/2}} + \dots \right) \psi_{R1}' \\
 &\quad + \left( \frac{1}{\sqrt{1 + \varepsilon_{iR}^2}} + \frac{\varepsilon_{iR}^2 \varepsilon_L^2}{(1 + \varepsilon_{iR}^2)^{5/2}} + \dots \right) t_{R2}, \quad (4.8)
 \end{aligned}$$

and similarly for the left- and right-handed  $b$ -quarks with  $\varepsilon_{iR} \rightarrow \varepsilon_{bR}$ . Here we denote the upper components of the  $SU(2)$  doublet fields as  $\psi_{L0,L1,R1}'$ ; clearly the smaller the value of  $\varepsilon_L$  ( $\varepsilon_{iR}$ ), the more strongly the left-handed (right-handed) eigenstate will be concentrated at site 0 (site 2). Note that the relative phase of the eigenvectors  $t_L$  and  $t_R$  is set by the eigenstate condition

$$M_i^\dagger |t_L\rangle = m_i |t_R\rangle. \quad (4.9)$$

The left- and right-handed heavy fermion mass eigenstates are the orthogonal combinations

$$\begin{aligned}
 T_L &= T_L^0 \psi_{L0}' + T_L^1 \psi_{L1}' \quad (4.10) \\
 &= \left( -\frac{\varepsilon_L}{1 + \varepsilon_{iR}^2} - \frac{(2\varepsilon_{iR}^2 - 1)\varepsilon_L^3}{2(\varepsilon_{iR}^2 + 1)^3} + \dots \right) \psi_{L0}' \\
 &\quad + \left( -1 + \frac{\varepsilon_L^2}{2(1 + \varepsilon_{iR}^2)^2} + \frac{(8\varepsilon_{iR}^2 - 3)\varepsilon_L^4}{8(\varepsilon_{iR}^2 + 1)^4} + \dots \right) \psi_{L1}' \quad (4.11)
 \end{aligned}$$

$$\begin{aligned}
 T_R &= T_R^1 \psi_{R1}' + T_R^2 t_{R2}, \quad (4.12) \\
 &= \left( -\frac{1}{\sqrt{1 + \varepsilon_{iR}^2}} - \frac{\varepsilon_{iR}^2 \varepsilon_L^2}{(1 + \varepsilon_{iR}^2)^{5/2}} + \dots \right) \psi_{R1}' \\
 &\quad + \left( -\frac{\varepsilon_{iR}}{\sqrt{1 + \varepsilon_{iR}^2}} + \frac{\varepsilon_{iR} \varepsilon_L^2}{(1 + \varepsilon_{iR}^2)^{5/2}} + \dots \right) t_{R2}, \quad (4.13)
 \end{aligned}$$

and similarly for the left- and right-handed heavy  $B$ -quarks with  $\varepsilon_{iR} \rightarrow \varepsilon_{bR}$ .

Analogous results follow for the other ordinary fermions and their heavy partners, with the appropriate  $\varepsilon_{fR}$  substituted for  $\varepsilon_{iR}$  in the expressions above.

### B. Ideal delocalization

As shown in [33] it is possible to minimize precision electroweak corrections due to the light fermions by appropriate (“ideal”) delocalization of the light fermions along the Moose. Essentially, if we recall that the  $W$  is orthogonal to its own heavy KK modes (the  $W'$  in the three-site model), then it is clear that relating the fermion profile along the Moose appropriately to the  $W$  profile can ensure that the  $W'$  will be unable to couple to the fermions. Specifically, at site  $i$  we require the couplings and wave functions of the ideally delocalized fermion and the  $W$

boson to be related as

$$g_i(\psi_i^f)^2 = g_W v_W^i. \quad (4.14)$$

In the three-site model, if we write the wave function of a delocalized left-handed fermion  $f_L = f_L^0 \psi_{L0}' + f_L^1 \psi_{L1}'$  then ideal delocalization imposes the following condition (having taken the ratio of the separate constraints for  $i = 0$  and  $i = 1$ ):

$$\frac{g(f_L^0)^2}{\tilde{g}(f_L^1)^2} = \frac{v_W^0}{v_W^1}. \quad (4.15)$$

Based on our general expressions for fermion mass eigenstates (Eqs. (4.7) and (4.8)) and the  $W$  mass eigenstate (3.3), it is clear that (4.15) relates the flavor-independent quantities  $x$  and  $\varepsilon_L$  to the flavor-specific  $\varepsilon_{fR}$ . Hence, if we construe this as an equation for  $\varepsilon_L$  and solve perturbatively in the small quantity  $x$ , we find<sup>3</sup>

$$\varepsilon_L^2 \rightarrow (1 + \varepsilon_{fR}^2)^2 \left[ \frac{x^2}{2} + \left( \frac{1}{8} - \frac{\varepsilon_{fR}^2}{2} \right) x^4 + \frac{5\varepsilon_{fR}^4 x^6}{8} + \dots \right]. \quad (4.16)$$

Regardless of the precise value of  $\varepsilon_{fR}$  involved, it is immediately clear that ideal delocalization implies  $\varepsilon_L = \mathcal{O}(x)$ . Since  $x \ll 1$ , this justifies the expansions used above in diagonalizing the fermion mass matrix.

The value of  $\varepsilon_L$  that yields precisely ideal delocalization for a given fermion species depends on  $\varepsilon_{fR}$  and therefore (4.4) on the fermion’s mass. For example, the value of  $\varepsilon_L$  that ideally delocalizes the  $b$  depends on  $\varepsilon_{bR}$ . As we will see below, however, bounds on the right-handed  $Wtb$  coupling will yield the constraint  $\varepsilon_{bR} \leq 1.4 \times 10^{-2}$ ; when Eq. (4.16) is applied to the  $b$ -quark and this constraint is imposed, terms proportional to  $\varepsilon_{bR}$  become negligible. As all other fermions (except top) are even lighter, the associated values of  $\varepsilon_{fR}$  will be even smaller. In practice, therefore, we may neglect all terms proportional to  $\varepsilon_{fR}$  in Eq. (4.16), and the condition for ideal mixing is essentially the same for all fermions except the top-quark:

$$\begin{aligned}
 \varepsilon_L^2 &= \frac{x^2}{2} + \frac{x^4}{8} + \mathcal{O}(x^8) \\
 &= 2 \left( \frac{M_W^2}{M_{W'}^2} \right) + 6 \left( \frac{M_W^2}{M_{W'}^2} \right)^2 + 22 \left( \frac{M_W^2}{M_{W'}^2} \right)^3 + \dots, \quad (4.17)
 \end{aligned}$$

where the second equality follows from Eq. (3.6). This is the value of  $\varepsilon_L$  we will henceforth use for all fermions in our analysis. As discussed in [35], we expect that the value of  $x$  will be bounded by constraints on the  $WWZ$  vertex when the light fermions are ideally delocalized.

<sup>3</sup>In the three-site model, this choice of  $\varepsilon_L^2$  is equivalent to a choice of the parameter  $b$  in [45] to make  $\varepsilon_3$  or  $\alpha S$  vanish.

## V. FERMION COUPLINGS TO THE $W$ BOSON

### A. Left-handed fermion couplings to the $W$ boson

We may now compute the couplings between left-handed fermions (ordinary or heavy partners) and the light  $W$  boson.<sup>4</sup> In terms of the mass-eigenstate gauge fields, the left-handed couplings of the light  $W$ 's may be written

$$\mathcal{L}_{WL} \propto W_\mu^+ [g v_W^0 (\bar{\psi}_{L0} \tau^- \gamma^\mu \psi_{L0}) + \tilde{g} v_W^1 (\bar{\psi}_{L1} \tau^- \gamma^\mu \psi_{L1})] + \text{H.c.} \quad (5.1)$$

The couplings of the light- $W$  to the mass-eigenstate fermions are then computed by decomposing the gauge-eigenstate fermions into mass-eigenstates.

We begin with the left-handed  $Wtb$  coupling, assuming ideal mixing for the  $b$ -quark in the  $\varepsilon_{bR} \rightarrow 0$  limit. Because the  $W$  wave function receives contributions from sites 0 and 1 only, the  $Wff'$  coupling is the sum of the overlap between the  $W$  and fermion wave functions on those two sites:

$$g_L^{Wtb} = g t_L^0 b_L^0 v_W^0 + \tilde{g} t_L^1 b_L^1 v_W^1; \quad (5.2)$$

we find

$$g_L^{Wtb} = g \left( 1 - \frac{3\varepsilon_{tR}^4 + 4\varepsilon_{tR}^2 + 3}{8(\varepsilon_{tR}^2 + 1)^2} x^2 + \frac{3\varepsilon_{tR}^8 + 16\varepsilon_{tR}^6 + 50\varepsilon_{tR}^4 + 8\varepsilon_{tR}^2 + 15}{128(\varepsilon_{tR}^2 + 1)^4} x^4 + \dots \right). \quad (5.3)$$

The corresponding equation for the coupling of standard-model fermions other than the top-quark to the  $W$  may be obtained by taking  $\varepsilon_{tR} \rightarrow 0$  in the equation above, yielding

$$g_L^W = g \left( 1 - \frac{3}{8} x^2 + \frac{15}{128} x^4 + \dots \right). \quad (5.4)$$

Combining this with Eqs. (2.4), (3.2), (3.9), and (3.10) we find

$$g_L^W = \frac{e}{\sqrt{1 - \frac{M_W^2}{M_Z^2}}} [1 + \mathcal{O}(s^2 x^4)], \quad (5.5)$$

which shows that the  $W$ -fermion couplings (for fermions other than top) are of very nearly standard-model form, as consistent with ideal delocalization. Eq. (5.4) corresponds to a value of  $G_F$

$$\sqrt{2} G_F = \frac{(g_L^W)^2}{4M_W^2} = \frac{1}{v^2} \left( 1 - \frac{x^2}{2} + \frac{x^4}{4} + \dots \right), \quad (5.6)$$

and the relation

<sup>4</sup>See also the BESS results [37].

$$g_L^{Wtb} = g_L^W \left( 1 + \frac{\varepsilon_{tR}^2}{4(\varepsilon_{tR}^2 + 1)^2} x^2 - \frac{\varepsilon_{tR}^2 (3\varepsilon_{tR}^6 + 8\varepsilon_{tR}^4 + 4\varepsilon_{tR}^2 + 10)}{32(\varepsilon_{tR}^2 + 1)^4} x^4 + \dots \right). \quad (5.7)$$

The  $W$  also couples to the heavy partners of the ordinary fermions. Here, we quote the results for the  $T$  and  $B$  fermions; analogous results follow for other generations when  $\varepsilon_{tR}$  is replaced by the appropriate  $\varepsilon_{qR}$ . There is a diagonal  $WTB$  coupling of the form

$$g_L^{WTB} = g T_L^0 B_L^0 v_W^0 + \tilde{g} T_L^1 B_L^1 v_W^1, \quad (5.8)$$

$$= \frac{g}{2} \left( 1 - \frac{\varepsilon_{tR}^4 - 6\varepsilon_{tR}^2 - 5}{8(\varepsilon_{tR}^2 + 1)^2} x^2 + \dots \right) \quad (5.9)$$

$$= \frac{g_L^W}{2} \left( 1 + \frac{\varepsilon_{tR}^4 + 6\varepsilon_{tR}^2 + 4}{4(\varepsilon_{tR}^2 + 1)^2} x^2 + \dots \right), \quad (5.10)$$

where  $T_L^{0,1}$  and  $B_L^{0,1}$  are the heavy-fermion analogs of the components  $t_L^{0,1}$  and  $b_L^{0,1}$ . There are also smaller off-diagonal couplings involving one heavy and one ordinary fermion

$$g_L^{WTb} = g T_L^0 b_L^0 v_W^0 + \tilde{g} T_L^1 b_L^1 v_W^1, \quad (5.11)$$

$$= \frac{g(1 - \varepsilon_{tR}^2)}{2\sqrt{2}(\varepsilon_{tR}^2 + 1)} (x + \mathcal{O}(x^3)), \quad (5.12)$$

and

$$g_L^{WtB} = g t_L^0 B_L^0 v_W^0 + \tilde{g} t_L^1 B_L^1 v_W^1, \quad (5.13)$$

$$= \frac{g(1 + 2\varepsilon_{tR}^2)}{2\sqrt{2}(\varepsilon_{tR}^2 + 1)} (x + \mathcal{O}(x^3)), \quad (5.14)$$

which play an important role in radiative corrections.

### B. Weak mixing angle

From Eqs. (3.9), (3.10), and (5.6) we can calculate the ‘‘Z standard’’ weak mixing angle<sup>5</sup>  $\theta_W|_Z$ :

$$s_Z^2 c_Z^2 \equiv \frac{e^2}{4\sqrt{2} G_F M_Z^2} = s^2 c^2 + s^2 (c^2 - s^2) \left( c^2 - \frac{1}{4} \right) x^2 + \mathcal{O}(x^4), \quad (5.15)$$

where  $s_Z \equiv \sin\theta_W|_Z$  and  $c_Z \equiv \cos\theta_W|_Z$ . The relationship between the weak mixing angle  $\theta_W|_Z$  and the angle  $\theta$  defined in Eq. (2.4) is expressed as follows:

$$s_Z^2 = s^2 + \Delta, \quad c_Z^2 = c^2 - \Delta, \quad (5.16)$$

<sup>5</sup>See also the BESS results [37,45].

$$\Delta \equiv s^2 \left( c^2 - \frac{1}{4} \right) x^2 + \mathcal{O}(x^4). \quad (5.17)$$

In other words,  $s^2$  and  $s_z^2$  differ by corrections of order  $x^2$ .

### C. Right-handed fermion couplings to the $W$ boson and $b \rightarrow s\gamma$

Because  $\psi_R$  is a doublet under  $SU(2)_1$ , the three-site model includes a right-handed coupling of the  $W$

$$\mathcal{L}_{WR} \propto W_\mu^+ [\tilde{g} v_W^1 (\bar{\psi}_{R1} \tau^- \gamma^\mu \psi_{R1})] + \text{H.c.} \quad (5.18)$$

Note that the right-handed fermions exist only on sites 1 and 2 while the  $W$  is limited to sites 0 and 1; hence, the right-handed coupling comes entirely from the overlap at site 1. For the  $tb$  doublet we find

$$g_R^{Wtb} = \tilde{g} t_R^1 b_R^1 v_W^1 \quad (5.19)$$

$$= \frac{g}{2} \frac{\varepsilon_{tR}}{\sqrt{1 + \varepsilon_{tR}^2}} \frac{\varepsilon_{bR}}{\sqrt{1 + \varepsilon_{bR}^2}} (1 + \mathcal{O}(x^2)) \quad (5.20)$$

$$\approx \frac{g}{2} \frac{m_b}{m_t} \frac{\varepsilon_{tR}^2}{1 + \varepsilon_{tR}^2}, \quad (5.21)$$

where reaching the last line requires use of Eq. (4.4). It is interesting to note that this expression is precisely analogous to the related expression in the continuum model (see Eq. (4.17) of [30]).

The right-handed  $Wtb$  coupling can yield potentially large contributions to  $b \rightarrow s\gamma$ . As shown in [50], agreement with the experimental upper limit on this process requires

$$\frac{g_R^{Wtb}}{g_L^W} < 4 \times 10^{-3}. \quad (5.22)$$

Combining this bound with our expressions for  $g_L^W$  (5.4) and  $g_R^{Wtb}$  (5.21), recalling  $x \ll 1$ , and using  $m_t = 175$  GeV,  $m_b = 4.5$  GeV, yields the constraint

$$\varepsilon_{tR} < 0.67. \quad (5.23)$$

As we shall see below, this constraint will automatically be satisfied for  $M > 1.8$  TeV—a mass limit that will be shown to be required for consistency with top-quark mass generation and limits on  $\varepsilon_L$ . Finally, combining Eqs. (4.4) and (5.23), reveals that

$$\varepsilon_{bR} < 1.4 \times 10^{-2}, \quad (5.24)$$

as referred to earlier. Again, this confirms that the same value of  $\varepsilon_L$  can produce nearly perfect ideal delocalization for the  $b$  and all of the lighter fermions.

The  $W$  also has right-handed couplings to  $T$  and  $B$ , for which we compute the diagonal coupling

$$g_R^{WTB} = \tilde{g} T_R^1 B_R^1 v_W^1 \quad (5.25)$$

$$= \frac{g}{2\sqrt{1 + \varepsilon_{tR}^2}} \left( 1 + \frac{\varepsilon_{tR}^4 + 6\varepsilon_{tR}^2 + 1}{8(\varepsilon_{tR}^2 + 1)^2} x^2 + \dots \right) \quad (5.26)$$

$$= \frac{g_L^W}{2\sqrt{1 + \varepsilon_{tR}^2}} \left( 1 + \frac{\varepsilon_{tR}^4 + 3\varepsilon_{tR}^2 + 1}{2(\varepsilon_{tR}^2 + 1)^2} x^2 + \dots \right), \quad (5.27)$$

and the off-diagonal coupling

$$g_R^{WtB} = \tilde{g} t_R^1 B_R^1 v_W^1 \quad (5.28)$$

$$= \frac{g \varepsilon_{tR}}{2\sqrt{1 + \varepsilon_{tR}^2}} \left( 1 + \frac{\varepsilon_{tR}^4 + 2\varepsilon_{tR}^2 - 3}{8(\varepsilon_{tR}^2 + 1)^2} x^2 + \dots \right) \quad (5.29)$$

$$= \frac{g_L^W \varepsilon_{tR}}{2\sqrt{1 + \varepsilon_{tR}^2}} \left( 1 + \frac{\varepsilon_{tR}^2 (\varepsilon_{tR}^2 + 2)}{2(\varepsilon_{tR}^2 + 1)^2} x^2 + \dots \right). \quad (5.30)$$

As in the case of  $g_R^{Wtb}$ , the right-handed coupling  $g_R^{WtB}$  turns out to be proportional to  $\varepsilon_{bR}$ , and is therefore very small.

Other right-handed  $Wqq'$  couplings involving the light standard fermions are straightforward to deduce from Eq. (5.20) and clearly suppressed by the small values of  $\varepsilon_{qR}$ . Similarly, the off-diagonal  $g_R^{WQq'}$  are proportional to small  $\varepsilon_{qR}$ . The diagonal  $g_R^{WQQ'}$  are analogous in form to (5.27).

## VI. FERMION COUPLINGS TO THE Z BOSON

The  $Z$  coupling to fermions may now be computed. Like the  $W$ , the  $Z$  may couple to a pair of ordinary or heavy-partner fermions, or to a mixed pair with one ordinary and one heavy-partner fermion. The left-handed coupling of the light  $Z$ -boson to quark fields may be written

$$\mathcal{L}_{ZL} \propto Z_\mu \left[ g v_Z^0 \left( \bar{\psi}_{L0} \frac{\tau^3}{2} \gamma^\mu \psi_{L0} \right) + \tilde{g} v_Z^1 \left( \bar{\psi}_{L1} \frac{\tau^3}{2} \gamma^\mu \psi_{L1} \right) + \frac{g'}{6} v_Z^2 \left( \bar{\psi}_{L0} \gamma^\mu \psi_{L0} + \bar{\psi}_{L1} \gamma^\mu \psi_{L1} \right) \right], \quad (6.1)$$

where the first two terms give rise to the left-handed “ $T_3$ ” coupling and the last term (proportional to  $g'$ ) gives rise to the left-handed hypercharge coupling. The expression for leptons would be similar, replacing hypercharge  $1/6$  with  $-1/2$ .

Similarly, the right-handed coupling of the  $Z$  to quark fields is

$$\mathcal{L}_{ZR} \propto Z_\mu \left[ \tilde{g} v_Z^1 \left( \bar{\psi}_{R1} \frac{\tau^3}{2} \gamma^\mu \psi_{R1} \right) + \frac{g'}{6} v_Z^2 \left( \bar{\psi}_{R1} \gamma^\mu \psi_{R1} \right) + g' v_Z^2 \left( \frac{2}{3} \bar{u}_{R2} \gamma^\mu u_{R2} - \frac{1}{3} \bar{d}_{R2} \gamma^\mu d_{R2} \right) \right], \quad (6.2)$$

where the last three terms arise from the hypercharge. For leptons,  $1/6 \rightarrow -1/2$  in the second term,  $2/3 \rightarrow 0$  in the

third term (for neutrinos), and  $-1/3 \rightarrow -1$  in the last term for the charged leptons. For quarks, this expression may be more conveniently rewritten as

$$\begin{aligned} \mathcal{L}_{ZR} \propto Z_\mu \left[ (\tilde{g}v_Z^1 - g'v_Z^2) \left( \bar{\psi}_{R1} \frac{\tau^3}{2} \gamma^\mu \psi_{R1} \right) \right. \\ \left. + g'v_Z^2 \left( \frac{2}{3} \sum_{i=1,2} \bar{u}_{Ri} \gamma^\mu u_{Ri} - \frac{1}{3} \sum_{i=1,2} \bar{d}_{Ri} \gamma^\mu d_{Ri} \right) \right], \end{aligned} \quad (6.3)$$

where the last two terms yield the  $Z$ -couplings to the conventionally defined right-handed hypercharge of the quarks, while the first can give rise to a new right-handed “ $T_3$ ” coupling.

### A. Light fermion couplings to the $Z$ boson

We now use Eqs. (6.1) and (6.3) to compute the couplings of the  $Z$  to light fermions. For an ideally localized light fermion  $f$ , we find the left-handed coupling to  $T_3$  by summing the overlaps of the  $Z$  and fermion wave functions on sites 0 and 1 (the loci of the  $T_3$  charges):

$$g_{3L}^{Zqq} = g(f_L^0)^2 v_Z^0 + \tilde{g}(f_L^1)^2 v_Z^1 \quad (6.4)$$

$$= gc \left( 1 - \frac{x^2 c^2 (3 + 6t^2 - t^4)}{8} + \dots \right) \quad (6.5)$$

$$= \frac{eM_W}{M_Z \sqrt{1 - \frac{M_W^2}{M_Z^2}}} [1 + \mathcal{O}(s^2 x^4)]. \quad (6.6)$$

The coupling of left-handed light fermions to hypercharge arises from the overlap between the fraction of the  $Z$  wave function arising from site 2 (the locus of hypercharge) and the left-handed fermion wave functions which are limited to sites 0 and 1:

$$g_{YL}^{Zqq} = g'v_Z^2 [(f_L^0)^2 + (f_L^1)^2] = g'v_Z^2 \quad (6.7)$$

$$= -g's \left( 1 + \frac{x^2 c^2 (3 - 2t^2 - t^4)}{8} + \dots \right) \quad (6.8)$$

$$= -\frac{eM_Z}{M_W} \sqrt{1 - \frac{M_W^2}{M_Z^2}} [1 + \mathcal{O}(s^2 x^4)]. \quad (6.9)$$

Eqs. (6.6) and (6.9), derived from the preceding equations using Eqs. (2.4), (3.2), (3.9), and (3.10) show that the couplings are very nearly of standard-model form; this is a further check of ideal delocalization.

Since the right-handed light fermion eigenvectors are localized entirely at site 2, there are no right-handed couplings of the light fermions to  $T_3$  and the right-handed hypercharge coupling of the  $Z$  is given by

$$g_{YR}^{Zqq} = g'v_Z^2 (f_R^2)^2 = g'v_Z^2 = g_{YL}^{Zqq}, \quad (6.10)$$

where the last equality comes from Eq. (6.7).

For ideally delocalized light fermions, therefore, we find the  $Z$ -couplings are given by the standard-model like expression

$$\frac{eM_Z}{M_W \sqrt{1 - \frac{M_W^2}{M_Z^2}}} \left( T_3 P_L - \left( 1 - \frac{M_W^2}{M_Z^2} \right) Q \right) [1 + \mathcal{O}(s^2 x^4)], \quad (6.11)$$

where  $P_L$  is the left-handed chirality projection operator.

### B. Top- and bottom-quark couplings to the $Z$ boson

The left-handed coupling of the top-quark to  $T_3$  is

$$g_{3L}^{Ztt} = g(t_L^0)^2 v_Z^0 + \tilde{g}(t_L^1)^2 v_Z^1 \quad (6.12)$$

$$= g_{3L}^{Zqq} \left( 1 + \frac{\varepsilon_{tR}^2 (2 + \varepsilon_{tR}^2)}{4c^2 (1 + \varepsilon_{tR}^2)^2} x^2 + \dots \right). \quad (6.13)$$

Note that a similar expression holds for the bottom-quark, with  $\varepsilon_{tR} \rightarrow \varepsilon_{bR}$  and therefore, from Eq. (5.24), the tree-level corrections to the partial width  $\Gamma(Z \rightarrow b\bar{b})$  are proportional to  $\varepsilon_{bR}^2/2 < 0.01\%$ . From Eqs. (6.1) and (6.3), we see that the left- and right-handed top-quark couplings to  $Y$  turn out to be the same as those for the other quarks

$$g_{YL}^{Ztt} = g'v_Z^2 [(t_L^0)^2 + (t_L^1)^2] = g_{YL}^{Zqq} \quad (6.14)$$

$$g_{YR}^{Ztt} = g'v_Z^2 [(t_R^1)^2 + (t_R^2)^2] = g_{YR}^{Zqq}. \quad (6.15)$$

We may also compute the right-handed  $T_3$  couplings of the top-quark

$$g_{3R}^{Ztt} = (\tilde{g}v_Z^1 - g'v_Z^2) (t_R^2)^2 \quad (6.16)$$

$$= \frac{g}{2c} \frac{\varepsilon_{tR}^2}{1 + \varepsilon_{tR}^2} (1 + \mathcal{O}(x^2)). \quad (6.17)$$

The  $T_3$  couplings of the  $Z$  to a pair of heavy-partner fermions or an off-diagonal pair are given in Table I. From the form of Eqs. (6.1) and (6.3), we see that the hypercharge couplings of the  $Z$  to a pair of left-handed or right-handed heavy-partner fermions follow the pattern of the ordinary fermions:

$$g_{YR}^{ZQQ} = g'v_Z^2 = g_{YL}^{ZQQ}, \quad (6.18)$$

and the hypercharge coupling of the  $Z$  to an off-diagonal (flavor-conserving)  $Qq$  pair always vanishes

$$g_{YL}^{ZQq} = g_{YR}^{ZQq} = 0, \quad (6.19)$$

because the  $Q$  and  $q$  wave functions are orthogonal.



TABLE I. Strength of the  $T_3$  portion of the  $Z$  coupling to top-flavored fermions in the three-site model to order  $x^3$ . The  $\varepsilon_{iR} \rightarrow \varepsilon_{fR}$  limit of a top-flavor coupling is the corresponding coupling of flavor  $f$ .

Coupling	Calculated as	Strength
$g_{3L}^{Zf}$	$g_0 v_Z^0 (t_L^0)^2 + g_1 v_Z^1 (t_L^1)^2$	$c g - \frac{1}{8} c^3 g (3 + 6t^2 - t^4) x^2 + \frac{g \varepsilon_{iR}^2 (2 + \varepsilon_{iR}^2)}{4c(1 + \varepsilon_{iR}^2)} x^2$
$g_{3R}^{Zf}$	$(g_1 v_Z^1 - g_2 v_Z^2) (t_R^1)^2$	$\frac{g \varepsilon_{iR}^2}{2c(\varepsilon_{iR}^2 + 1)} \left(1 + \frac{-3(\varepsilon_{iR}^2 + 1)^2 + 8c^2 \varepsilon_{iR}^2 (\varepsilon_{iR}^2 + 2) - 4c^4 (\varepsilon_{iR}^2 + 1)^2}{8c^2 (\varepsilon_{iR}^2 + 1)^2} x^2\right)$
$g_{3L}^{ZTT}$	$g_0 v_Z^0 (T_L^0)^2 + g_1 v_Z^1 (T_L^1)^2$	$-\frac{1}{2} c g (t^2 - 1) + \frac{c g (4(t^2 + 1) - c^2 (\varepsilon_{iR}^2 + 1)^2 (t^2 - 1)^3)}{16c^3 (\varepsilon_{iR}^2 + 1)^2} x^2$
$g_{3R}^{ZTT}$	$(g_1 v_Z^1 - g_2 v_Z^2) (T_R^1)^2$	$\frac{g}{2c(\varepsilon_{iR}^2 + 1)} + g \frac{(-3(\varepsilon_{iR}^2 + 1)^2 + 8c^2 (\varepsilon_{iR}^4 + 3\varepsilon_{iR}^2 + 1) - 4c^4 (\varepsilon_{iR}^2 + 1)^2)}{16c^3 (\varepsilon_{iR}^2 + 1)^3} x^2$
$g_{3L}^{ZfT}$	$g_0 v_Z^0 t_L^0 T_L^0 + g_1 v_Z^1 t_L^1 T_L^1$	$\frac{g}{2\sqrt{2}c(\varepsilon_{iR}^2 + 1)} x + g \frac{((\varepsilon_{iR}^2 + 1)^2 + c^2 (\varepsilon_{iR}^4 + 6\varepsilon_{iR}^2 - 3) - 4c^4 (\varepsilon_{iR}^2 + 1)^2)}{16\sqrt{2}c^3 (\varepsilon_{iR}^2 + 1)^3} x^3$
$g_{3R}^{ZfT}$	$(g_1 v_Z^1 - g_2 v_Z^2) t_R^1 T_R^1$	$\frac{g \varepsilon_{iR}}{2c(\varepsilon_{iR}^2 + 1)} + g \varepsilon_{iR} \frac{(-3(\varepsilon_{iR}^2 + 1)^2 + 4c^2 (2\varepsilon_{iR}^4 + 5\varepsilon_{iR}^2 + 1) - 4c^4 (\varepsilon_{iR}^2 + 1)^2)}{16c^3 (\varepsilon_{iR}^2 + 1)^3} x^2$

## VII. IMPLICATIONS OF MULTIPLE GAUGE-BOSON COUPLINGS

### A. ZWW Vertex and $\varepsilon_L$

Experimental constraints on the  $ZWW$  vertex in the three-site model turn out to provide useful bounds on the fermion delocalization parameter  $\varepsilon_L$ .

To leading order, in the absence of  $CP$ -violation, the triple gauge-boson vertices may be written in the Hagiwara-Peccei-Zeppenfeld-Hikasa triple gauge vertex notation [51]

$$\begin{aligned}
\mathcal{L}_{TGV} = & -ie \frac{c_Z}{s_Z} [1 + \Delta\kappa_Z] W_\mu^+ W_\nu^- Z^{\mu\nu} \\
& - ie [1 + \Delta\kappa_\gamma] W_\mu^+ W_\nu^- A^{\mu\nu} \\
& - ie \frac{c_Z}{s_Z} [1 + \Delta g_1^Z] (W^{+\mu\nu} W_\mu^- - W^{-\mu\nu} W_\mu^+) Z_\nu \\
& - ie (W^{+\mu\nu} W_\mu^- - W^{-\mu\nu} W_\mu^+) A_\nu, \quad (7.1)
\end{aligned}$$

where the two-index tensors denote the Lorentz field-strength tensor of the corresponding field. In the standard model,  $\Delta\kappa_Z = \Delta\kappa_\gamma = \Delta g_1^Z \equiv 0$ .

As noted in ref. [35], in any vector-resonance model, such as the Higgsless models considered here, the interactions (7.1) come from re-expressing the non-Abelian couplings in the kinetic energy terms in the original Lagrangian in terms of the mass-eigenstate fields. In this case one obtains equal contributions to the deviations of the first and third terms, and the second and fourth terms in Eq. (7.1). In addition the coefficient of the fourth term is fixed by electromagnetic gauge invariance, and therefore in these models we find

$$\Delta\kappa_\gamma \equiv 0 \quad \Delta\kappa_Z \equiv \Delta g_1^Z. \quad (7.2)$$

Computing the  $ZWW$  coupling explicitly in the three-site model<sup>6</sup> yields

$$g_{ZWW} = g(v_W^0)^2 v_Z^0 + \tilde{g}(v_W^1)^2 v_Z^1 \quad (7.3)$$

$$= g c \left(1 - \frac{x^2 c^2 (1 + 2t^2 - t^4)}{4} + \dots\right) \quad (7.4)$$

$$= e \frac{c_Z}{s_Z} \left(1 + \frac{1}{8c^2} x^2 + O(x^4)\right) \quad (7.5)$$

$$= g_{3L}^{Zqq} \left(1 + \frac{x^2}{8c^2} + \dots\right), \quad (7.6)$$

where Eq. (7.5) is derived using (5.17). Hence we compute

$$\Delta g_1^Z = \Delta\kappa_Z = \frac{x^2}{8c^2} > 0. \quad (7.7)$$

The 95% C.L. upper limit from LEP-II is  $\Delta g_1^Z < 0.028$  [53]. Approximating  $c^2 \approx \cos^2 \theta_W \approx 0.77$ , we find the bound on  $x$

$$x \leq 0.42 \sqrt{\frac{\Delta g_1^Z}{0.028}}, \quad (7.8)$$

and hence, from Eq. (3.5),

$$M_{W'} \approx \frac{2}{x} M_W \geq 380 \text{ GeV} \sqrt{\frac{0.028}{\Delta g_1^Z}}. \quad (7.9)$$

From Eq. (4.17), therefore, we can write

$$\varepsilon_L = \frac{m}{M} \approx \frac{x}{\sqrt{2}} \approx 0.30 \left(\frac{380 \text{ GeV}}{M_{W'}}\right). \quad (7.10)$$

Finally, we recall that, in the absence of a Higgs boson,  $W_L W_L$  spin-0 isospin-0 scattering would violate unitarity at a scale of  $\sqrt{8\pi}v$  and that exchange of the heavy electroweak bosons is what unitarizes  $WW$  scattering in Higgsless models. Hence,  $M_{W'} \leq 1.2 \text{ TeV}$  in the three-site model. This constrains  $\varepsilon_L$  to lie in the range

$$0.095 \leq \varepsilon_L \leq 0.30. \quad (7.11)$$

<sup>6</sup>See also the BESS results [45,52].

TABLE II. Quantities related to multi-gauge-boson vertices and chiral Lagrangian parameters in the three-site model and the continuum model of Ref [35].

	Three-site model	Continuum model
$\Delta g_1^Z = \Delta \kappa_Z$	$\frac{1}{2c^2} \left( \frac{M_W^2}{M_{W'}^2} \right)$	$\frac{\pi^2}{12c^2} \left( \frac{M_W^2}{M_{W'}^2} \right)$
$\Delta g_{WWWW}$	$\frac{5}{4} \left( \frac{M_W^2}{M_{W'}^2} \right)$	$\frac{\pi^2}{5} \left( \frac{M_W^2}{M_{W'}^2} \right)$
$e^2 \alpha_1$	0	0
$e^2 \alpha_2 = -e^2 \alpha_3$	$-\frac{s^2}{2} \left( \frac{M_W^2}{M_{W'}^2} \right)$	$-\frac{\pi^2 s^2}{12} \left( \frac{M_W^2}{M_{W'}^2} \right)$
$e^2 \alpha_4 = -e^2 \alpha_5$	$\frac{s^2}{4} \left( \frac{M_W^2}{M_{W'}^2} \right)$	$\frac{\pi^2 s^2}{30} \left( \frac{M_W^2}{M_{W'}^2} \right)$

From Eq. (3.4) the bounds on  $M_{W'}$  may be translated directly to bounds on the size of  $\tilde{g}$ , yielding

$$0.19 < \frac{\tilde{g}^2}{4\pi} < 1.9 \ll 4\pi. \quad (7.12)$$

Hence we see that  $SU(2)_1$  is moderately strongly coupled, with radiative corrections (which are proportional to  $\tilde{g}^2/(4\pi)^2$ ) of order 20%.

### B. Comparison to the continuum model

The three-site model may be viewed as an extremely deconstructed version of the model studied in Ref. [35]: a five-dimensional flat-space  $SU(2)_A \otimes SU(2)_B$  gauge theory with ideally delocalized fermions. Hence it is interesting to compare the values of the multiple gauge-boson and chiral Lagrangian parameters obtained for the two cases.

The limit of the continuum model that is related to the three-site model has the bulk gauge couplings of  $SU(2)_A$  and  $SU(2)_B$ ,  $g_{5A}$  and  $g_{5B}$ , equal to one another; in the notation of Ref. [35],  $\kappa = \frac{g_{5B}^2}{g_{5A}^2} = 1$ . Then, we may express both the values of the chiral Lagrangian parameters  $\alpha_i$  for the three-site model (see Appendix) and those from Ref. [35] in terms of the mass ratio  $M_W^2/M_{W'}^2$ , as shown in Table II. Note that  $\Delta g_{WWWW}$  in the table is defined by

$$g_{WWWW} = \frac{e^2}{s_Z^2} [1 + \Delta g_{WWWW}]. \quad (7.13)$$

If we fix the value of  $\left(\frac{M_W^2}{M_{W'}^2}\right)$ , the quantities listed in Table II for the three-site model are about 70% as large as those for the continuum model.

## VIII. PHENOMENOLOGICAL BOUNDS

### A. Corrections to $\alpha T$

At leading order, there are two isospin-violating parameters [24,25] of interest. These may be chosen [25] to be  $\Delta\rho$ , the deviation from one of the ratio of the strengths of low-energy isotriplet neutral- and charged-current neutrino interactions, and  $\alpha T$ , isospin-violating corrections to the masses of the electroweak bosons [21–23]. Because of

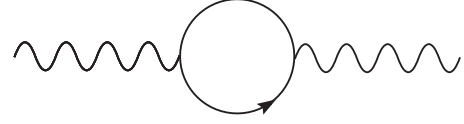


FIG. 2. One-loop contributions to  $\Delta\rho$  arise from the differences in the vacuum polarization diagram for the  $W^3$  versus  $W^{1,2}$ . We compute the leading contribution in the limit  $\varepsilon_L \rightarrow 0$  and  $m_b \rightarrow 0$  (and  $g' \rightarrow 0$ ).

the custodial symmetry present in the limit  $g' \rightarrow 0$ , at tree level  $\Delta\rho$  is always equal to zero and  $\alpha T$  is small ( $\mathcal{O}(x^4)$ ) in models of this kind [15,18].

The existence of the new  $T$  and  $B$  fermions, the heavy partners of the top and bottom, gives rise to new one-loop contributions to  $\alpha T$ , as illustrated in Fig. 2. In principle, it is the sum of the SM ( $t$  and  $b$ -quark loops) and new physics contributions that is finite. However, we note that the SM contribution vanishes in the limit  $\varepsilon_L \rightarrow 0$  (and  $g' \rightarrow 0$ ) since the  $t$  and  $b$ -quark masses are then equal (both vanish, per Eq. (4.2)). Since  $\varepsilon_L$  respects custodial symmetry, and fermionic custodial symmetry violation is encoded in the  $\varepsilon_{fR}$  coefficients, we may obtain the leading contribution to  $\alpha T$  from the new physics by performing the calculation in the  $\varepsilon_L \rightarrow 0$  limit. We obtain

$$\alpha T \approx \frac{1}{16\pi^2} \frac{m_t^4}{M^2 v^2} = \frac{1}{16\pi^2} \frac{\varepsilon_{tR}^4 M^2}{v^2}. \quad (8.1)$$

Since  $g' \neq 0$ , there are also isospin-violating corrections at one-loop in the gauge sector which yield corrections to  $\alpha T$  of order  $\alpha/4\pi$ . The  $M_{W'}$  dependence of the largest of these corrections, which are proportional to  $\log(M_{W'}^2/M_W^2)$ , exactly matches [54] the Higgs boson mass dependence of isospin-violating contributions at one-loop in the standard model. Hence in the three-site model, to leading-log approximation, the role of the Higgs boson is largely played by the  $W'$ .<sup>7</sup>

The phenomenological bounds on the value of  $\alpha T$  depend (since they include the one-loop SM corrections) on the reference Higgs mass chosen. We are therefore interested in the bounds on  $\alpha T$  corresponding to Higgs masses between about 380 GeV (from Eq. (7.9)) and the unitarity bound 1.2 TeV. Current bounds (see, for example, Langacker and Eler in [56]) yield (approximately)  $\alpha T \leq 2.5 \times 10^{-3}$ , at 90% confidence level, assuming the existence of a moderately heavy (340 GeV) Higgs boson, while it is relaxed to approximately  $\alpha T \leq 5 \times 10^{-3}$  in the case of a heavy (1000 GeV) Higgs boson. We therefore expect that the upper bound on  $\alpha T$  in the three-site model varies

<sup>7</sup>At one-loop, a heavy SM Higgs boson requires an additional positive contribution to  $\alpha T$  to bring it into agreement with precision electroweak data. To the extent that the tree-level values of  $\alpha S$  and  $\alpha T$  are precisely zero, similar considerations can allow one to set a lower bound on  $\alpha T$  in the three-site model as a function of  $M_{W'}$  [55]. This, in turn, would provide an upper bound on the Dirac mass of the heavy fermions.

from approximately  $2.5 \times 10^{-3}$  to  $5 \times 10^{-3}$ . We may rewrite Eq. (8.1) as

$$\varepsilon_{tR} = 0.79 \left( \frac{\alpha T}{2.5 \times 10^{-3}} \right)^{1/4} \left( \frac{v}{M} \right)^{1/2}. \quad (8.2)$$

In what follows, we will quote limits on the parameters of the model for both of these values. For  $\alpha T = 5 \times 10^{-3}$ , we find the upper bound

$$\varepsilon_{tR} < 0.94 \left( \frac{v}{M} \right)^{1/2}. \quad (8.3)$$

As we shall see shortly, this bound is stronger than the one derived from  $b \rightarrow s\gamma$ .

### B. Bounds on $M$

Our upper limit on  $\varepsilon_{tR}$  and our knowledge of the top-quark mass allow us to derive a lower bound on  $M$ . Our expression (4.3) for  $m_t$  reminds us that

$$m_t \approx \frac{mm'_t}{\sqrt{M^2 + m_t'^2}} = \frac{\varepsilon_L \varepsilon_{tR} M}{\sqrt{1 + \varepsilon_{tR}^2}}. \quad (8.4)$$

For a given value of  $M$ , the existence of an upper bound on  $\varepsilon_{tR}$  implies that there is a *smallest* allowed value of  $\varepsilon_L$ , which we denote  $\varepsilon_L^*$

$$\varepsilon_L^* = 1.26 \left( \frac{2.5 \times 10^{-3}}{\alpha T} \right)^{1/4} \frac{m_t}{\sqrt{vM}} \times \sqrt{1 + 0.63 \left( \frac{\alpha T}{2.5 \times 10^{-3}} \right)^{1/2} \frac{v}{M}}. \quad (8.5)$$

Since Eq. (7.11) requires  $\varepsilon_L^* < 0.30$ , for  $\alpha T = 2.5 \times 10^{-3}$  we find that  $M$  must be greater than 2.3 TeV, and for  $\alpha T = 5 \times 10^{-3}$  we find that  $M$  must be greater than 1.8 TeV.

Several additional consequences follow. Using  $M > 1.8$  TeV and the bound in Eq. (8.3), we see that  $\varepsilon_{tR} < 0.35$ , which supersedes the  $b \rightarrow s\gamma$  constraint, Eq. (5.23), as promised above. For  $\alpha T = 2.5 \times 10^{-3}$ , as  $M$  grows above its minimum value of 2.3 TeV, according to Eq. (8.5) the value of  $\varepsilon_L^*$  will fall—reaching the lower bound of 0.095 (Eq. (7.11)) when  $M \approx 22$  TeV. For values of  $M$  greater than 22 TeV (and fixed  $m_t$ ), the entire range of  $0.095 < \varepsilon_L < 0.30$  remains accessible if  $\varepsilon_{tR}$  is smaller than its maximum value (which, for  $\alpha T = 2.5 \times 10^{-3}$ , is 0.26). The joint range of allowed  $\varepsilon_L$  and  $M$  for both values of  $\alpha T$  is summarized in Figs. 3 and 4.

In the simplest continuum models in which the fifth dimension is a flat interval, the mass of the first KK fermion resonance is approximately half of the mass of the first gauge-boson KK resonance. Because of the chiral boundary conditions on the fermions, Dirichlet at one boundary and Neumann at the other, the lowest KK fermion mode has a wavelength of twice the size of the 5-d interval. Phenomenologically, this situation is disfavored—and it has been suggested that this may be ad-

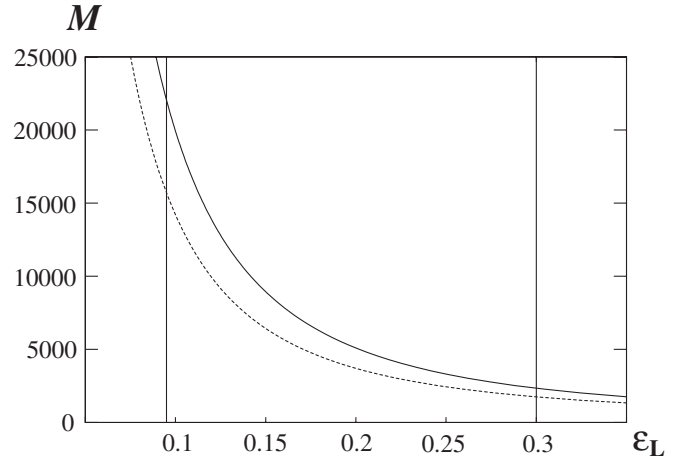


FIG. 3. Phenomenologically acceptable values of  $M$  in GeV and  $\varepsilon_L$  for  $\alpha T = 2.5 \times 10^{-3}$  (solid curve) and  $5 \times 10^{-3}$  (dashed curve). The region bounded by the lines  $0.095 < \varepsilon_L < 0.30$ , and above the appropriate curve is allowed. For a given  $M$  and  $\varepsilon_L$ , the value of  $\varepsilon_{tR}$  is determined by Eq. (8.4). As discussed in the text, naive dimensional analysis implies  $M < 46$  TeV.

dressed by having the fermions “feel” a smaller size for the 5-d interval than the gauge bosons [28,30]. Following [30], the parameter which measures this enhancement is then given by

$$2 \frac{m_{t^*}}{M_{W'}}, \quad (8.6)$$

and, for the three-site model, we find its minimum value is about 12 for  $\alpha T = 2.5 \times 10^{-3}$  and 7 for  $\alpha T = 5 \times 10^{-3}$ . In other words, viewing the three-site model as the deconstruction of a continuum one, the bulk fermion fields

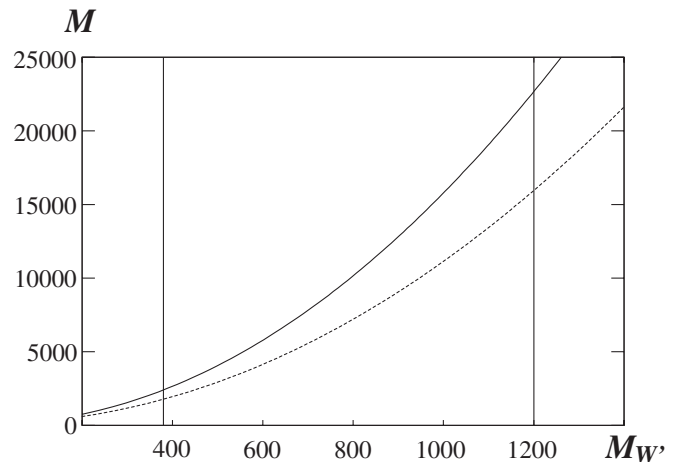


FIG. 4. Phenomenologically acceptable values of  $M$  and  $M_{W'}$  in GeV for  $\alpha T = 2.5 \times 10^{-3}$  (solid curve) and  $5 \times 10^{-3}$  (dashed curve). The region bounded by the lines  $380 \text{ GeV} < M_{W'} < 1200 \text{ GeV}$  and above the curve are allowed. For a given  $M$  and  $M_{W'}$  (see Eq. (7.10)), the value of  $\varepsilon_{tR}$  is determined by Eq. (8.4). As discussed in the text, naive dimensional analysis implies  $M < 46$  TeV.

behave as though the 5-d interval is at least 12 or 7 times smaller than do the gauge bosons.

It is interesting to ask what *upper* bound exists on  $M$ . From the expression for the fermion mass matrix in Eq. (4.1) we have

$$M = \frac{\sqrt{2}\lambda v}{\varepsilon_L}. \quad (8.7)$$

Eq. (7.11) requires  $\varepsilon_L \geq 0.095$ , and from naive dimensional analysis or, equivalently, perturbative unitarity, we expect  $\lambda \leq 4\pi$ . Hence,  $M < 46$  TeV. A more sophisticated analysis could be done by imposing unitarity of  $WW \rightarrow t\bar{t}$ , as in [30] (see also, footnote 7).

### IX. DECOUPLING AND $Z \rightarrow b\bar{b}$ WITH A TOY UV COMPLETION

In the analysis above we have argued that the “bulk fermion” Dirac mass  $M$  in the three-site model must be large, between 1.8 and 46 TeV. Such a mass is potentially much larger than  $4\pi\sqrt{2}v \approx 4.3$  TeV, the largest mass which can arise from the symmetry breaking encoded by the link fields. By contrast, the nonlinear sigma-model link fields have so far been described by an effective chiral Lagrangian which is valid only at energies *less* than of order  $4\pi\sqrt{2}v$ . In order to discuss the three-site model in the large- $M$  limit, therefore, one must consider the question in the context of a theory which is consistent to much higher scales—e.g. a renormalizable one. The situation here is similar to the consistent analysis [57] of the Appelquist-Chanowitz bound [58].

The simplest possible renormalizable extension of the three-site model is formed by promoting the link fields in Fig. 1 to linear sigma-model fields. Here one introduces two additional singlet fields  $H_i$  ( $i = 1, 2$ ) and considers the matrix fields

$$\Phi_i = \frac{(H_i + f_i)}{2} \Sigma_i, \quad (9.1)$$

which transform as  $(2, \bar{2})$  under the appropriate  $SU(2)$ ’s, and which have the kinetic energy terms

$$\text{Tr}(D^\mu \Phi_i^\dagger D_\mu \Phi_i) \rightarrow \frac{1}{2} \partial^\mu H_i \partial_\mu H_i + \frac{f_i^2}{4} \text{Tr}(D^\mu \Sigma_i^\dagger D_\mu \Sigma_i). \quad (9.2)$$

The most general renormalizable potential for the fields  $\Phi_{1,2}$  will result in mixing between the fields  $H_{1,2}$ , which will therefore not be mass eigenstates. For the purposes of this note, however, this will not be relevant—we will require that, consistent with dimensional analysis, the masses of the “Higgs” are bounded by  $4\pi\sqrt{2}v$ .

For completeness, in this section we will carry the explicit dependence on  $f_{1,2}$ , although in practice we always have in mind  $f_1 \simeq f_2 \simeq \sqrt{2}v$  (as in Eq. (2.2)). We continue

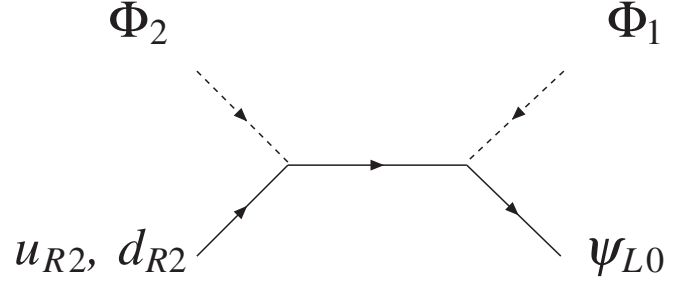


FIG. 5. Mass-mixing diagram which yields the operator in Eq. (9.5) when integrating out the bulk fermion (interior fermion line) at tree level.

to work in the limit in which  $x = g_0/g_1 \ll 1$  and  $y = g_2/g_1 \ll 1$ .

In this linear sigma-model version of the three-site model, the Yukawa couplings and fermion mass term are of the form below, which is the natural extension of Eq. (2.1)

$$\begin{aligned} \mathcal{L}_f = & \varepsilon_L M \left( 1 + \frac{H_1}{f_1} \right) \bar{\psi}_{L0} \Sigma_1 \psi_{R1} + M \bar{\psi}_{R1} \psi_{L1} \\ & + M \left( 1 + \frac{H_2}{f_2} \right) \bar{\psi}_{L1} \Sigma_2 \begin{pmatrix} \varepsilon_{uR} & \\ & \varepsilon_{dR} \end{pmatrix} \begin{pmatrix} u_{R2} \\ d_{R2} \end{pmatrix} + \text{H.c.} \end{aligned} \quad (9.3)$$

Although the Yukawa couplings are written in terms of the Dirac mass  $M$  for convenience, we do impose (see the discussion surrounding Eq. (8.7)) the consistency constraint

$$\frac{\varepsilon_L M}{f_1}, \frac{(\varepsilon_{uR}, \varepsilon_{dR}) M}{f_2} < 4\pi, \quad (9.4)$$

on the size of the allowed Yukawa couplings.

#### A. The large $M$ effective theory

We now consider the large- $M$  limit. Because of the decoupling theorem [59], the effects of the bulk (i.e., site-1) fermion on low-energy parameters must be suppressed by powers of  $M$ . Because of the parameterization of the couplings chosen in Eq. (9.3), the form of the operators in the low-energy effective theory may not obviously appear to be suppressed by  $M$  when written in terms of the parameters  $\varepsilon_L$  and  $\varepsilon_{uR,dR}$ . Nonetheless, because of the constraints of Eq. (9.4), the effects of the bulk fermion always formally decouple in the  $M \rightarrow \infty$  limit [59]. We will now look at light-fermion masses, the coupling of delocalized light fermions to gauge bosons, and  $\alpha T$  in the large- $M$  limit and see how the results compare with our previous findings.

##### 1. Light-fermion masses

The masses of the ordinary fermions arise in the large- $M$  limit when we consider the diagram connecting left-

handed (site-0) and right-handed (site-2) brane fermions in Fig. 5 and then integrate out the intervening site-1 bulk fermion at tree level. Specifically, this gives rise to the operator:

$$\mathcal{L}'_f \propto \frac{\varepsilon_L M}{f_1 f_2} \bar{\psi}_{L0} \Phi_1 \Phi_2 \begin{pmatrix} \varepsilon_{uR} & \\ & \varepsilon_{dR} \end{pmatrix} \begin{pmatrix} u_{R2} \\ d_{R2} \end{pmatrix} + \text{H.c.} \quad (9.5)$$

$$\propto \varepsilon_L M \left(1 + \frac{H_1}{f_1}\right) \left(1 + \frac{H_2}{f_2}\right) \bar{\psi}_{L0} \Sigma_1 \Sigma_2 \begin{pmatrix} \varepsilon_{uR} & \\ & \varepsilon_{dR} \end{pmatrix} \begin{pmatrix} u_{R2} \\ d_{R2} \end{pmatrix} + \text{H.c.} \quad (9.6)$$

In unitary gauge (with  $\Sigma_i = I$ ) the leading term provides the up-type fermion with a mass of the typical see-saw form  $m_u \propto \varepsilon_L \varepsilon_{uR} M$  that agrees with Eq. (4.2), and similarly for the down-type fermion. The overall power of  $M$  results from two powers of  $M$  in the Yukawa couplings, and one factor of  $1/M$  from the propagator in Fig. 5.

### 2. Ideally delocalized fermion couplings

In this limit, it should also be possible to obtain an effective coupling of  $\psi_{L0}$  to the  $SU(2)$  group at site 1, consistent with light-fermion delocalization. Indeed, considering Fig. 6 and integrating out the bulk fermion at tree level induces the operator

$$\mathcal{L}'_{Wff} \propto \frac{\varepsilon_L^2}{f_1^2} \bar{\psi}_{L0} \Phi_1 i \not{D} \Phi_1^\dagger \psi_{L0}, \quad (9.7)$$

$$\supset \varepsilon_L^2 \bar{\psi}_{L0} \Sigma_1 i \not{D} \Sigma_1^\dagger \psi_{L0}, \quad (9.8)$$

which includes (easily visible in unitary gauge) just such an effective coupling. In this case, the two powers of  $M$  in the Yukawa couplings are canceled by  $1/M^2$  from the fermion propagators in Fig. 6. If we adjust the value of the coefficient  $\varepsilon_L$  to make the coupling of the light fermions to the  $W'$  vanish, we achieve ideal delocalization of the light fermions. The coupling of the brane fermions to the bulk gauge group is then precisely of the form discussed in [33,45].

### 3. Deviations in $\alpha T$

We may also check that the size of  $\alpha T$  in the large- $M$  limit is consistent with our previous calculation. As discussed in Section VIII A, we expect that the leading contributions from beyond-the-standard-model physics will persist in the  $\varepsilon_L \rightarrow 0$  limit and will arise, in fact, from the weak-isospin violation encoded in the  $\varepsilon_{fR}$ . Then the appropriate diagram<sup>8</sup> involves only the  $\bar{\psi}_{L1} \Phi_2(u_{R2}, d_{R2})$  Yukawa couplings in Eq. (9.3) as shown in Fig. 7, and gives rise to the operator<sup>9</sup>

<sup>8</sup>See [60] for a similar analysis in the case of the top-quark see-saw model.

<sup>9</sup>One may also deduce that this is the leading operator by recalling that  $\alpha T$  violates weak isospin by two units. An isotriplet operator would not suffice.

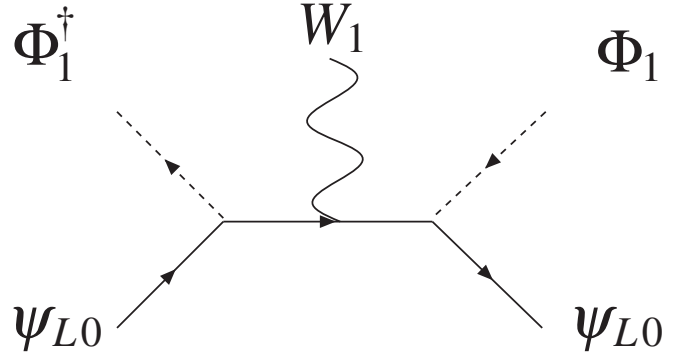


FIG. 6. Coupling diagram which yields the operator in Eq. (9.7) when integrating out the bulk fermion at tree level.

$$\mathcal{L}'_{\Delta\rho} \propto \frac{M^2}{16\pi^2 f_2^4} \left( \text{Tr} \begin{pmatrix} \varepsilon_{uR}^2 & \\ & \varepsilon_{dR}^2 \end{pmatrix} \Phi_2^\dagger D^\mu \Phi_2 \right)^2, \quad (9.9)$$

$$\propto \frac{M^2}{16\pi^2} \left( \text{Tr} \begin{pmatrix} \varepsilon_{uR}^2 & \\ & \varepsilon_{dR}^2 \end{pmatrix} \Sigma_2^\dagger D^\mu \Sigma_2 \right)^2. \quad (9.10)$$

In unitary gauge, this may be seen to affect the mass of the  $Z$  and not that of the  $W$ . It encodes the very corrections to  $\alpha T$  discussed in Section VIII A and Eq. (8.1). Here the  $M^2$  arises from four powers of  $\varepsilon_R M$  from the couplings and an overall  $1/M^2$  from the convergent loop integral in the diagram.

### B. $Z \rightarrow b\bar{b}$

With this background, we may now discuss flavor-dependent corrections to the process  $Z \rightarrow b\bar{b}$ . We will do so in the limit that  $m_b = 0$ , and hence  $\varepsilon_{bR} = 0$ . In the large- $M$  limit, therefore, we are interested in flavor-dependent corrections to the coupling of the lower component of  $\psi_{L0}$  to the  $SU(2)_0$  gauge bosons. Furthermore, as we are interested in flavor-nonuniversal contributions, we are only interested in couplings proportional to  $\varepsilon_{iR}$ —any contributions depending only on  $\varepsilon_L$  will be flavor-universal.

There are no relevant contributions at tree level, as the neutral gauge-boson couplings involving  $\varepsilon_{iR}$  at tree level couple to the upper component of  $\psi_{L0}$ —i.e., to the top-quark. The leading contributions arise from diagrams of the form shown in Fig. 8. Note that the diagram involves the exchange of a charged Goldstone boson (necessary to couple to the lower component of  $\psi_{L0}$ ), two couplings proportional to  $\varepsilon_L$ , and two proportional to  $\varepsilon_{iR}$ . This diagram, and those like it, give rise to the low-energy operator

$$\mathcal{L}_{Zbb} \propto \frac{\varepsilon_L^2}{16\pi^2 f_1^2 f_2^2} \sum_a \bar{\psi}_{L0} \left[ \left( \frac{\tau^a}{2} \right) \Phi_1^\dagger \not{D} \Phi_2^\dagger \begin{pmatrix} \varepsilon_{uR}^2 & \\ & \varepsilon_{dR}^2 \end{pmatrix} \right. \\ \left. \times \Phi_2 \Phi_1 \left( \frac{\tau^a}{2} \right) \right] \psi_{L0}. \quad (9.11)$$

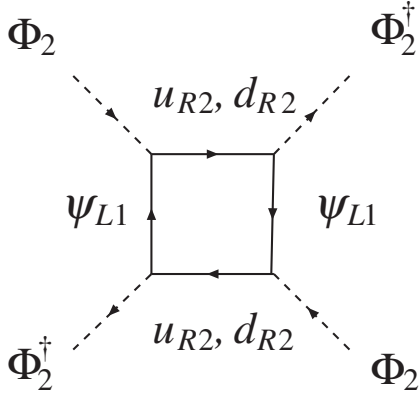


FIG. 7. Loop diagram giving the leading contribution to  $\alpha T$ , as encoded in the operator of Eq. (9.9).

Here four powers of  $M$  from the Yukawa couplings are canceled by  $1/M^4$  from dimensional analysis.

An operator of this sort gives rise to a shift in the  $Zbb$  coupling of order

$$\frac{\delta g_{Zbb}}{g_{Zbb}^{SM}} \propto \frac{\varepsilon_L^2 \varepsilon_{iR}^2}{16\pi^2} = \frac{m_i^2}{16\pi^2 M^2}. \quad (9.12)$$

By contrast, the one-loop SM contribution to the  $Zb\bar{b}$  coupling [61,62] is of order  $m_i^2/16\pi^2 v^2$ . We therefore see that the new corrections to the process  $Z \rightarrow b\bar{b}$  arising in the three-site model are likely, even for the lowest possible  $M$ , to be negligibly small!6

In models with an extra dimension, one might generally be worried about effects which arise from integrating out the KK modes [63], as shown in Fig. 9. Integrating out the heavy  $W'$  would lead one to anticipate a relatively large contribution of the form

$$\frac{\delta g_{Zbb}}{g_{Zbb}^{SM}} \simeq \frac{g^2 v^2}{16\pi^2 M_{W'}^2} \log\left(\frac{M_{W'}^2}{m_t^2}\right). \quad (9.13)$$

In a theory with ideal delocalization, however, the  $W'tb$  coupling vanishes, and therefore there is no such effect in the three-site model described here.

We should also note that the estimate given above provides only a lower bound on the size of the corrections to the  $Zb\bar{b}$  coupling. It is possible that in a truly dynamical model, the “extended technicolor”-like physics responsible for generating the Yukawa couplings can give rise to new contributions [64].

Finally, it is worth mentioning that the situation could be somewhat different in a model with “Georgi fermions” [65]. In this case, all of the fermion masses arise from dimension-four Yukawa couplings so that it is not possible to take the large- $M$  limit, even in principle. Nonetheless, the analysis given here, taking the limit  $M \rightarrow \mathcal{O}(4\pi v)$ , shows that the effects on  $Z \rightarrow b\bar{b}$  are still likely to be quite small.

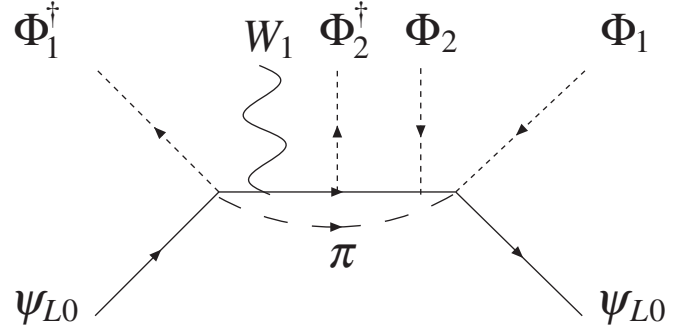


FIG. 8. Loop diagram giving leading contribution to the non-universal correction to  $Z \rightarrow b\bar{b}$ . Here  $\pi$  corresponds to a quantum charged “eaten” Goldstone boson, and the vertex involving the fermions,  $\Phi_1^\dagger$  and  $\pi$  is to be interpreted using the “background field” method to preserve chiral invariance. This diagram, and those like it, give rise to the operator in Eq. (9.11) in the low-energy theory.

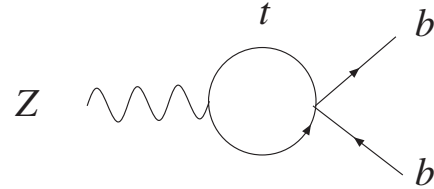


FIG. 9. A potentially large correction to  $Z \rightarrow b\bar{b}$  in extra-dimensional models [63]. Because of ideal delocalization, however, the  $W'tb$  coupling vanishes, and this contribution is small in the three-site model described here.

## X. CONCLUSIONS

The three-site model is a useful tool for illustrating many issues of current interest in Higgsless models: ideal fermion delocalization, precision electroweak corrections, fermion mass generation, and phenomenological constraints. Because the Moose describing the model has only one interior  $SU(2)$  group, there is, accordingly, only a single triplet of  $W'$  and  $Z'$  states instead of the infinite tower of triplets present in the continuum limit. Likewise, there need only be a single heavy-fermion partner for each of the standard-model fermions, instead of a tower of such states. Because the  $W'$  and  $Z'$  states are fermiophobic when the light fermions are ideally delocalized, discovering these heavy gauge bosons at a high-energy collider will require careful study of gauge-boson fusion processes [35,66]. Fortunately, the sparse spectrum and limited number of model parameters should allow this model to be encoded in a Matrix Element Generator program in concert with a Monte Carlo Event Generator for detailed phenomenological investigations.

In this paper, we have discussed the forms of the gauge-boson and fermion wave functions and their couplings to one another, and then explored the phenomenological implications. We established the form of the fermion Yukawa

couplings required to produce the ideal fermion delocalization that causes tree-level precision electroweak corrections to vanish by making the  $W'$  and  $Z'$  fermiophobic. We discussed the implications of corrections to multi-gauge-boson vertices for ideal delocalization, and compared the sizes of electroweak chiral Lagrangian parameters in the three-site model with those for the continuum limit. In addition, we have studied a variety of phenomenological constraints arising from anomalous gauge couplings, and from one-loop corrections to  $b \rightarrow s\gamma$  and the weak-isospin-violating parameter  $\alpha T$ . We found that the extra fermiophobic vector boson states (the analogs of the gauge-boson KK modes in a continuum model) can be reasonably light, with a mass as low as 380 GeV, while the extra (approximately vectorial) quark and lepton states must satisfy  $1.8 \text{ TeV} \leq M \leq 46 \text{ TeV}$ .

Because the bulk fermion's Dirac mass  $M$  does not arise from electroweak symmetry breaking, its effects on low-energy parameters must decouple. To investigate this explicitly, we have constructed a large- $M$  effective field theory. Since  $M$  lies above the range of validity of the nonrenormalizable nonlinear sigma model for the link fields, our analysis employs the simplest possible UV completion, in which the link fields are given by renormalizable linear sigma models. This allows us to construct an effective low-energy theory produced when the bulk fermions of mass  $M$  are integrated out. We confirmed that the results in the large- $M$  effective theory for the top-quark mass, the gauge-boson couplings required by ideal delocalization, and the one-loop contribution to  $\alpha T$  are precisely those we computed directly. We then used the large- $M$  effective theory to estimate the size of the nonuniversal corrections to the  $Zb\bar{b}$  coupling—and found that these corrections can be very small, proportional to  $m_t^2/16\pi^2 M^2$ .

### ACKNOWLEDGMENTS

R. S. C., E. H. S., B. C., and S. D. are supported in part by the US National Science Foundation under grant No. PHY-0354226. M. T.'s work is supported in part by the JSPS Grant-in-Aid for Scientific Research No. 16540226. H. J. H. is supported by Tsinghua University. M. K. is supported in part by the US National Science Foundation under grant No. PHY-0354776. R. S. C. and E. H. S. thank the Aspen Center for Physics for its hospitality while this work was being completed.

### APPENDIX: FOUR-POINT GAUGE VERTICES AND CHIRAL LAGRANGIAN PARAMETERS

This appendix gives expressions for chiral Lagrangian parameters and the quartic  $W$  boson coupling for the three-site model in the notation used in this paper. These quantities have previously been derived for the equivalent gauge sector of the BESS model in [45,67].

Of the complete set of 12 CP-conserving operators in the electroweak chiral Lagrangian written down by Longhitano [68–73] and Appelquist and Wu [74], only five apply to Higgsless models such as the three-site model (see Ref. [35] for a discussion):

$$\mathcal{L}_1 \equiv \frac{1}{2} \alpha_1 g_W g_Y B_{\mu\nu} \text{Tr}(TW^{\mu\nu}) \quad (\text{A1})$$

$$\mathcal{L}_2 \equiv \frac{1}{2} i \alpha_2 g_Y B_{\mu\nu} \text{Tr}(T[V^\mu, V^\nu]) \quad (\text{A2})$$

$$\mathcal{L}_3 \equiv i \alpha_3 g_W \text{Tr}(W_{\mu\nu}[V^\mu, V^\nu]) \quad (\text{A3})$$

$$\mathcal{L}_4 \equiv \alpha_4 [\text{Tr}(V^\mu V^\nu)]^2 \quad (\text{A4})$$

$$\mathcal{L}_5 \equiv \alpha_5 [\text{Tr}(V_\mu V^\mu)]^2. \quad (\text{A5})$$

Here  $W_{\mu\nu}, B_{\mu\nu}, T \equiv U\tau_3 U^\dagger$ , and  $V_\mu \equiv (D_\mu U)U^\dagger$  are the basis of the expansion, with  $U$  being the nonlinear sigma-model field<sup>10</sup> arising from  $SU(2)_L \otimes SU(2)_R \rightarrow SU(2)_V$ . An alternative parametrization by Gasser and Leutwyler [75] names these coefficients as  $\alpha_1 = L_{10}$ ,  $\alpha_2 = -\frac{1}{2}L_{9R}$ ,  $\alpha_3 = -\frac{1}{2}L_{9L}$ ,  $\alpha_4 = L_2$ ,  $\alpha_5 = L_1$ .

The chiral Lagrangian coefficients are related<sup>11</sup> to  $\alpha S$ , the Hagiwara-Peccei-Zeppenfeld-Hikasa [51] triple-gauge vertex parameters and the quartic  $W$  boson vertex as follows [35]:

$$\alpha S = -(16\pi\alpha)\alpha_1, \quad (\text{A6})$$

$$\Delta g_1^Z = \frac{1}{c^2(c^2 - s^2)} e^2 \alpha_1 + \frac{1}{s^2 c^2} e^2 \alpha_3, \quad (\text{A7})$$

$$\Delta \kappa_Z = \frac{2}{(c^2 - s^2)} e^2 \alpha_1 - \frac{1}{c^2} e^2 \alpha_2 + \frac{1}{s^2} e^2 \alpha_3, \quad (\text{A8})$$

$$g_{WWWW} = \frac{e^2}{s_Z^2} \left[ 1 + \frac{2}{(c^2 - s^2)} e^2 \alpha_1 + \frac{2}{s^2} e^2 \alpha_3 + \frac{1}{s^2} e^2 \alpha_4 \right]. \quad (\text{A9})$$

An expression for  $g_{WWWW}$  may be calculated as follows:

$$\begin{aligned} g_{WWWW} &= g^2 (v_W^0)^4 + \tilde{g}^2 (v_W^1)^4 \\ &= g^2 \left( 1 - \frac{7}{16} x^2 + O(x^4) \right). \end{aligned} \quad (\text{A10})$$

Using Eq. (5.17) we may re-express this as

$$g_{WWWW} = \frac{e^2}{s_Z^2} \left( 1 + \frac{5}{16} x^2 + O(x^4) \right). \quad (\text{A11})$$

<sup>10</sup> $SU(2)_W \equiv SU(2)_L$  and  $U(1)_Y$  is identified with the  $T_3$  part of  $SU(2)_R$ .

<sup>11</sup> $\Delta \kappa_\gamma (= 0) = \frac{1}{s^2} (-e^2 \alpha_1 + e^2 \alpha_2 + e^2 \alpha_3)$  is automatically satisfied when  $\Delta g_1^Z = \Delta \kappa_Z$ .

Solving the relations in (A6)–(A9) using  $S = O(x^4)$ , the values of  $\Delta g_1^Z$  and  $\Delta \kappa_Z$  from the main text, and  $g_{WWWW}$  as above, we obtain:

$$e^2 \alpha_1 = O(x^4), \quad (\text{A12})$$

$$e^2 \alpha_2 = -e^2 \alpha_3 = -\frac{s^2}{8} x^2 + O(x^4), \quad (\text{A13})$$

$$e^2 \alpha_4 = -e^2 \alpha_5 = \frac{s^2}{16} x^2 + O(x^4). \quad (\text{A14})$$

The coefficients  $\alpha_4$  and  $\alpha_5$  provide the leading corrections to  $WW$  and  $WZ$  elastic scattering. Note that the three-site model has  $\alpha_2 \neq \alpha_3$  and therefore,  $L_{9L} \neq L_{9R}$  [35,73].

- 
- [1] C. Csaki, C. Grojean, H. Murayama, L. Pilo, and J. Terning, *Phys. Rev. D* **69**, 055006 (2004).
- [2] P. W. Higgs, *Phys. Lett.* **12**, 132 (1964).
- [3] K. Agashe, A. Delgado, M. J. May, and R. Sundrum, *J. High Energy Phys.* 08 (2003) 050.
- [4] C. Csaki, C. Grojean, L. Pilo, and J. Terning, *Phys. Rev. Lett.* **92**, 101802 (2004).
- [5] G. Burdman and Y. Nomura, *Phys. Rev. D* **69**, 115013 (2004).
- [6] G. Cacciapaglia, C. Csaki, C. Grojean, and J. Terning, *Phys. Rev. D* **70**, 075014 (2004).
- [7] I. Antoniadis, *Phys. Lett. B* **246**, 377 (1990).
- [8] R. Sekhar Chivukula, D. A. Dicus, and H.-J. He, *Phys. Lett. B* **525**, 175 (2002).
- [9] R. S. Chivukula and H.-J. He, *Phys. Lett. B* **532**, 121 (2002).
- [10] R. S. Chivukula, D. A. Dicus, H.-J. He, and S. Nandi, *Phys. Lett. B* **562**, 109 (2003).
- [11] H.-J. He, hep-ph/0412113.
- [12] R. Foadi, S. Gopalakrishna, and C. Schmidt, *J. High Energy Phys.* 03 042 (2004).
- [13] J. Hirn and J. Stern, *Eur. Phys. J. C* **34**, 447 (2004).
- [14] R. Casalbuoni, S. De Curtis, and D. Dominici, *Phys. Rev. D* **70**, 055010 (2004).
- [15] R. S. Chivukula, E. H. Simmons, H. J. He, M. Kurachi, and M. Tanabashi, *Phys. Rev. D* **70**, 075008 (2004).
- [16] M. Perelstein, *J. High Energy Phys.* 10 (2004) 010.
- [17] H. Georgi, *Phys. Rev. D* **71**, 015016 (2005).
- [18] R. Sekhar Chivukula, E. H. Simmons, H. J. He, M. Kurachi, and M. Tanabashi, *Phys. Rev. D* **71**, 035007 (2005).
- [19] N. Arkani-Hamed, A. G. Cohen, and H. Georgi, *Phys. Rev. Lett.* **86**, 4757 (2001).
- [20] C. T. Hill, S. Pokorski, and J. Wang, *Phys. Rev. D* **64**, 105005 (2001).
- [21] M. E. Peskin and T. Takeuchi, *Phys. Rev. D* **46**, 381 (1992).
- [22] G. Altarelli and R. Barbieri, *Phys. Lett. B* **253**, 161 (1991).
- [23] G. Altarelli, R. Barbieri, and S. Jadach, *Nucl. Phys. B* **369**, 3 (1992).
- [24] R. Barbieri, A. Pomarol, R. Rattazzi, and A. Strumia, *Nucl. Phys. B* **703**, 127 (2004).
- [25] R. S. Chivukula, E. H. Simmons, H.-J. He, M. Kurachi, and M. Tanabashi, *Phys. Lett. B* **603**, 210 (2004).
- [26] H. Georgi, *Nucl. Phys. B* **266**, 274 (1986).
- [27] G. Cacciapaglia, C. Csaki, C. Grojean, and J. Terning, *Phys. Rev. D* **71**, 035015 (2005).
- [28] G. Cacciapaglia, C. Csaki, C. Grojean, M. Reece, and J. Terning, *Phys. Rev. D* **72**, 095018 (2005).
- [29] R. Foadi, S. Gopalakrishna, and C. Schmidt, *Phys. Lett. B* **606**, 157 (2005).
- [30] R. Foadi and C. Schmidt, *Phys. Rev. D* **73**, 075011 (2006).
- [31] R. S. Chivukula, E. H. Simmons, H. J. He, M. Kurachi, and M. Tanabashi, *Phys. Rev. D* **71**, 115001 (2005).
- [32] R. Casalbuoni, S. De Curtis, D. Dolce and D. Dominici, *Phys. Rev. D* **71**, 075015 (2005).
- [33] R. Sekhar Chivukula, E. H. Simmons, H. J. He, M. Kurachi, and M. Tanabashi, *Phys. Rev. D* **72**, 015008 (2005).
- [34] R. Sekhar Chivukula, E. H. Simmons, H. J. He, M. Kurachi, and M. Tanabashi, *Phys. Rev. D* **72**, 095013 (2005).
- [35] R. S. Chivukula, E. H. Simmons, H. J. He, M. Kurachi, and M. Tanabashi, *Phys. Rev. D* **72**, 075012 (2005).
- [36] C. Grojean, W. Skiba, and J. Terning, *Phys. Rev. D* **73**, 075008 (2006).
- [37] R. Casalbuoni, S. De Curtis, D. Dominici, and R. Gatto, *Phys. Lett. B* **155**, 95 (1985).
- [38] R. Casalbuoni *et al.*, *Phys. Rev. D* **53**, 5201 (1996).
- [39] M. Bando, T. Kugo, S. Uehara, K. Yamawaki, and T. Yanagida, *Phys. Rev. Lett.* **54**, 1215 (1985).
- [40] M. Bando, T. Kugo, and K. Yamawaki, *Nucl. Phys. B* **259**, 493 (1985).
- [41] M. Bando, T. Fujiwara, and K. Yamawaki, *Prog. Theor. Phys.* **79**, 1140 (1988).
- [42] M. Bando, T. Kugo, and K. Yamawaki, *Phys. Rep.* **164**, 217 (1988).
- [43] M. Harada and K. Yamawaki, *Phys. Rep.* **381**, 1 (2003).
- [44] C. T. Hill and A. K. Leibovich, *Phys. Rev. D* **66**, 075010 (2002).
- [45] L. Anichini, R. Casalbuoni, and S. De Curtis, *Phys. Lett. B* **348**, 521 (1995).
- [46] J. M. Maldacena, *Adv. Theor. Math. Phys.* **2**, 231 (1998).
- [47] S. S. Gubser, I. R. Klebanov, and A. M. Polyakov, *Phys. Lett. B* **428**, 105 (1998).
- [48] E. Witten, *Adv. Theor. Math. Phys.* **2**, 253 (1998).
- [49] O. Aharony, S. S. Gubser, J. M. Maldacena, H. Ooguri, and Y. Oz, *Phys. Rep.* **323**, 183 (2000).
- [50] F. Larios, M. A. Perez, and C. P. Yuan, *Phys. Lett. B* **457**, 334 (1999).



- [51] K. Hagiwara, R. D. Peccei, D. Zeppenfeld, and K. Hikasa, Nucl. Phys. B **282**, 253 (1987).
- [52] R. Casalbuoni, S. De Curtis, and D. Guetta, Phys. Rev. D **55**, 4203 (1997).
- [53] ALEPH, DELPHI, L3, OPAL, and LEP TGC Working Group (The LEP Collaborations), LEPEWWG/TC/2005-01, 2005.
- [54] S. Matsuzaki, R. S. Chivukula, and E. H. Simmons, hep-ph/0607191.
- [55] R. S. Chivukula *et al.*, “Three-site model phenomenology” (unpublished).
- [56] S. Eidelman *et al.* (Particle Data Group), Phys. Lett. B **592**, 1 (2004).
- [57] M. Golden, Phys. Lett. B **338**, 295 (1994).
- [58] T. Appelquist and M. S. Chanowitz, Phys. Rev. Lett. **59**, 2405 (1987); **60**, 1589(E) (1988).
- [59] T. Appelquist and J. Carazzone, Phys. Rev. D **11**, 2856 (1975).
- [60] H. Collins, A. K. Grant, and H. Georgi, Phys. Rev. D **61**, 055002 (2000).
- [61] R. Barbieri, M. Beccaria, P. Ciafaloni, G. Curci, and A. Vicere, Phys. Lett. B **288**, 95 (1992); **312**, 511(E) (1993).
- [62] R. Barbieri, M. Beccaria, P. Ciafaloni, G. Curci, and A. Vicere, Nucl. Phys. B **409**, 105 (1993).
- [63] J. F. Oliver, J. Papavassiliou, and A. Santamaria, Phys. Rev. D **67**, 056002 (2003).
- [64] R. S. Chivukula, S. B. Selipsky, and E. H. Simmons, Phys. Rev. Lett. **69**, 575 (1992).
- [65] H. Georgi, hep-ph/0508014.
- [66] A. Birkedal, K. Matchev, and M. Perelstein, Phys. Rev. Lett. **94**, 191803 (2005).
- [67] R. Casalbuoni, S. De Curtis, and D. Dominici, Phys. Lett. B **403**, 86 (1997).
- [68] T. Appelquist and C. W. Bernard, Phys. Rev. D **22**, 200 (1980).
- [69] A. C. Longhitano, Phys. Rev. D **22**, 1166 (1980).
- [70] A. C. Longhitano, Nucl. Phys. B **188**, 118 (1981).
- [71] T. Appelquist, YALE Print-80-0832, 1980.
- [72] B. Holdom, Phys. Lett. B **258**, 156 (1991).
- [73] A. F. Falk, M. E. Luke, and E. H. Simmons, Nucl. Phys. B **365**, 523 (1991).
- [74] T. Appelquist and G. H. Wu, Phys. Rev. D **48**, 3235 (1993).
- [75] J. Gasser and H. Leutwyler, Ann. Phys. (N.Y.) **158**, 142 (1984).